SWI/SNF chromatin remodeling controls Notch-responsive enhancer accessibility

Zoe Pillidge[1] and Sarah J Bray[1]*

[1] Dept. of Physiology, Development and Neuroscience,
University of Cambridge,
Downing Street,
Cambridge,
CB2 3DY, UK

* Corresponding author

Running title: SWI/SNF control of Notch response

Word Count: 5350 including Abstract, Introduction, Results, Discussion, Figure Legends (35,512 characters including spaces).

Abstract

Notch signaling plays a key role in many cell fate decisions during development by directing different gene expression programs via the transcription factor CSL, known as Su(H) in *Drosophila.* Which target genes are responsive to Notch signaling is influenced by the chromatin state of enhancers, yet how this is regulated is not fully known. Detecting a specific increase in the histone variant H3.3 in response to Notch signaling, we tested which chromatin remodelers or histone chaperones are required for the changes in enhancer accessibility to Su(H) binding. We show a crucial role for the Brahma SWI/SNF chromatin remodeling complex, including the actin-related BAP55 subunit, in conferring enhancer accessibility and enabling the transcriptional response to Notch activity. The Notch-responsive regions have high levels of nucleosome turnover which depend on the Brahma complex, increase in magnitude with Notch signaling and primarily involve histone H3.3. Together these results highlight the importance of SWI/SNF-mediated nucleosome turnover in rendering enhancers responsive to Notch.

Key words: *Drosophila* / Histone H3.3 / Notch / Nucleosome turnover / SWI/SNF.

Introduction

Many cell fate decisions during development are directed by Notch signaling between neighboring cells, and misregulation of the pathway results in a variety of complex diseases [1,2]. Notch, the receptor, becomes cleaved upon binding to cell-surface ligands, freeing the Notch intracellular domain (NICD) to travel directly to the nucleus and activate target gene expression. Depending on the context, different genes are targeted by the Notch transcription complex due to differential enhancer accessibility [3–5]. Furthermore, successful activation involves largescale changes in histone modifications and chromatin accessibility across the target enhancers [4,6–8]. How these changes in chromatin structure are brought about remains to be determined.

The conserved DNA binding partner of NICD is known as Suppressor of Hairless (Su(H)) in *Drosophila melanogaster* or CSL more generally. In the absence of Notch activity, Su(H) partners with co-repressive proteins to prevent transcription, often acting on the same genes which are induced upon Notch signal activation [5]. The switch from genes being repressed (Notch-OFF) to activated (Notch-ON) involves a change in the dynamics of Su(H) binding, so that it acquires a longer residence time when participating in the activating complex, as well as increased accessibility of the DNA [8]. Several histone acetyltransferases and methyltransferases contribute to this switch [8–10] and their actions could explain some of the changes in histone post-translational modifications that have been observed [4,6,7]. However, the histone modifiers that have been identified do not explain how target enhancer accessibility is regulated, making it likely that other factors contribute.

One way that chromatin structure can be altered is by a change in the density or dynamics of the nucleosomes, coordinated by chromatin remodeling complexes which fall into four categories based on the classification of their ATPase domains: Imitation Switch (ISWI), Chromodomain helicase DNA-binding (CHD), Inositol-Requiring Protein 80 (INO80) and Switching-Defective/Sucrose Non-Fermenting (SWI/SNF) complexes [11–13]. Their common property of DNA translocation provides the force needed to dislodge histone-DNA contacts and is tailored to achieve nucleosome repositioning, sliding, ejection or editing depending on the complex [14]. Chromatin remodeling has been shown to facilitate gene expression in a variety of contexts. For example, INO80 is recruited by Oct4 at pluripotency genes to maintain their accessibility in ES cells [15], and by reducing nucleosome occupancy, it facilitates oncogene transcription in melanoma [16]. Similarly, SWI/SNF remodelers establish accessible enhancers in fibroblasts following their recruitment by lineage-specific transcription factors and FOS/JUN [17], and function to shift nucleosomes away from GATA1 sites in hematopoietic stem cells allowing TAL1-dependent transcription [18]. Conversely, in some cases chromatin remodeling can be inhibitory, such as at the MMLV promoter where SWI/SNF recruitment by the glucocorticoid receptor (GR) subsequently inhibits GR binding [19,20]. These diverse roles are highlighted by the fact that mutations affecting remodeling complexes can both promote and suppress tumor progression [11,21].

The contribution made by chromatin remodeling to Notch-dependent transcription is also unclear, as conflicting models have been proposed depending on the system and the type of analysis. For example, while two developmental studies based on genetics and phenotypic

analysis argued that SWI/SNF complexes contribute positively to Notch-dependent transcription [22,23], another proposed an inhibitory effect, detecting increased expression of a key target gene when SWI/SNF components were depleted [24]. Confounding the situation further, a non-nuclear effect on Notch trafficking was reported following depletion of Snr1, a member of SWI/SNF complexes in *Drosophila* [25]. It is possible that histone variants also play a role in regulating enhancer accessibility, and a recent study suggests that the acetylation of histone H2A.Z by Tip60 supports Notch-dependent gene expression [10]. However, none of these studies have analyzed the effects on chromatin dynamics directly, making it important to investigate how depletion of chromatin remodelers can bring about these effects on Notch-dependent transcription mechanistically.

Given that enhancer accessibility appears to play a key role in Notch-mediated transcription, we set out to investigate the nucleosome dynamics at target enhancers and to distinguish which chromatin remodelers are critical for enabling target gene activation by Notch. Firstly, we find that Notch signaling regulates nucleosome turnover at target enhancers and promotes incorporation of the histone variant H3.3. Secondly, by testing several classes of chromatin remodelers, we find that the BRM SWI/SNF complex, including the actin-related BAP55 subunit, is required for nucleosome turnover and the enhancer accessibility required for the Notch response. Thus, SWI/SNF complexes are vital for the Notch response, and we propose a model whereby dynamic chromatin remodeling poises Notch-responsive genes and facilitates their rapid activation.

Results

Ectopic Notch signaling increases the local concentration of histone H3.3 at the E(spl)-C

Previous work has shown that Notch signaling promotes largescale changes in chromatin structure, including rapid increases in histone acetylation and increased chromatin accessibility [4,6–8]. In *Drosophila*, these changes have been most clearly observed at the *Enhancer of split-Complex* (*E(spl)-C*), a 60kb region where 11 highly Notch-responsive genes are concentrated [26–29]. We therefore chose to investigate whether there are any largescale changes in the histone variant H3.3 or canonical histone H3 occupancy at this region following Notch activation, making use of a live tag marking the *E(spl)-C* in *Drosophila* larval salivary glands [8]. Without Notch signaling, both histones H3.3-GFP and H3-GFP were present at low levels at the *E(spl)-C* compared to surrounding regions. However, when we activated Notch signaling in this tissue by expressing a constitutively-active form of the Notch receptor, $N^{\Delta ECD}$ [30,31], under control of the GAL4/UAS system, the levels of H3.3-GFP were strongly increased compared to surrounding regions (Fig 1A, Notch-ON). This pattern was found to be reproducible when the relative fluorescence intensity was quantified across the locus in images taken from live salivary glands (Fig 1B). No such change was detected when we examined the effects on histone H3 in a similar manner (Fig 1C and D).

Histone H3.3 has been associated with actively-transcribed genes and can be incorporated into the chromatin independently of DNA replication [32,33]. To verify that the Notch-dependent increase in H3.3-GFP was replication-independent, we used a mutant form of histone H3.3, $H3.3^{core}$-GFP, which is only incorporated in a replication-independent manner [32]. Indeed, with $H3.3^{core}$-GFP we saw the same pattern as with H3.3-GFP (Fig 1E and F), suggesting that the local increase in histone H3.3 concentration at the *E(spl)-C* is not due to an increased level of endoreplication at this locus, and thus likely represents changes associated with Notch-induced transcription. Furthermore, when histone H3.3 tagged with another fluorophore, mKO, was expressed on a much shorter timescale under Notch-OFF and Notch-ON conditions, making use of a heat-shock-inducible FRT construct [34], the same pattern of incorporation was observed (Fig EV1). This showed that the incorporation of histone H3.3 under Notch-ON conditions is dynamic and ongoing during the period of Notch activity.

The BRM chromatin remodeling complex is required for Notch-responsive accessibility

The incorporation of histone H3.3 at Notch-regulated genes, along with the previously detected changes in accessibility [8], suggest an involvement of chromatin remodeling complexes and/or histone chaperones. In order to ascertain which of these are needed, we tested if any remodelers or chaperones are required for the recruitment of Su(H) to the *E(spl)-C.* We have previously shown that Notch activity promotes robust recruitment of Su(H)-GFP, detectable as a band of fluorescence when salivary gland nuclei are imaged live under conditions of UAS-$N^{\Delta ECD}$ expression (Fig 2A) [8]. We therefore performed RNAi knockdown of different chromatin remodelers and histone chaperones and assessed the impact on Su(H) recruitment under these Notch-ON conditions. To verify that the RNAi lines

were effective, RNA was extracted from the salivary glands and expression levels quantified by reverse transcription-qPCR (Fig EV2A). Only those chromatin remodelers and chaperones where a reduced expression was detected were analyzed further. In the majority of cases we detected little or no change in Su(H) recruitment (Fig 2A and B). For example, knockdown of components in the ISWI, NuRD and INO80 complexes failed to perturb Su(H) recruitment (for review of chromatin remodelers in *Drosophila,* see [35]). Likewise, knockdown of chromatin assembly factors or H3.3-specific chaperones such as DEK [36] or Yemanuclein (YEM) [37] had no effect. In contrast, depletion of core components of the BRM (BAF/PBAF) SWI/SNF chromatin remodeling complex [38,39] had a striking effect. Knockdown of Moira (SMARCC1/2) eliminated visible recruitment of Su(H)-GFP in all nuclei, while knockdown of Snr1 (SMARCB1) prevented the formation of a single clear band of recruitment in most nuclei (Fig 2A-D).

Expression of a commonly-used dominant negative form of the Brahma ATPase BrmK804R [40] had the same effect as Moira knockdown, preventing formation of the Su(H)-GFP band (Fig 2C and D). This demonstrates that the ATPase activity of the BRM complex is required for Su(H) recruitment. Furthermore, DNA staining of salivary gland nuclei showed that the chromosomes retained their characteristic DNA banding patterns, although the chromosomes were somewhat reduced in size (Fig EV2C). Thus, there was no global disruption to the nuclear architecture when BrmK804R was expressed, suggesting that the effects on Su(H) recruitment were specific.

Two different BRM complexes have been reported, BAP and PBAP (BAF and PBAF), which are distinguished by specific subunits OSA (ARIID1A/B) in BAP or BAP170 (ARID2) and Polybromo (PBRM1) in PBAP [38,39]. Surprisingly, these subunits do not appear to be essential for Notch-dependent Su(H) recruitment. A robust band of Su(H)-GFP was still detectable in nuclei depleted for OSA, BAP170 or Polybromo (Fig 2C and D), even though little or no detectable RNA or protein remained (Fig EV2B, D-G). This suggests that either the two complexes can compensate for each other or that the specialized subunits are not necessary for the Notch-mediated effects on chromatin.

Su(H) recruitment in the Notch-ON condition correlates with increased chromatin accessibility [8]. We therefore used the assay for transposase-accessible chromatin (ATAC) [41] to determine whether the BRM complex is required for this Notch-induced change, using qPCR to analyze different regions of the *E(spl)-C* (chosen regions illustrated in Fig 3A). Expression of BrmK804R had a very localized effect on accessibility measured with ATAC, causing a strong reduction at the *E(spl)mβ-HLH* and *E(spl)m3-HLH* enhancer regions in both Notch-OFF (Fig 3B) and Notch-ON (Fig 3C) conditions. The effects in the Notch-ON condition were the most dramatic, with BrmK804R largely abolishing the increases in accessibility induced by Notch across the *E(spl)-C* so that the locus resembled that in the Notch-OFF condition.

To determine whether the BRM complex plays the same role at other inducible enhancers, several additional regions were analyzed, including heat-shock and ecdysone-responsive regions. In contrast to the Notch-responsive regions in the *E(spl)*-C, the ecdysone-responsive regions of *Hr4, Dip-B* and *Eip75B* showed no decrease in accessibility in the presence of

BrmK804R (Fig EV3A and B) and, unlike *E(spl)mβ-HLH* and *E(spl)mα-HLH*, there was no decrease in transcription of these genes (Fig EV3C). Surprisingly, two heat-shock promoters underwent an increase in accessibility when BrmK804R was expressed (Fig EV3A and B). These data suggest that SWI/SNF chromatin remodeling complexes are differentially deployed depending on the regulatory mechanisms operating, and demonstrate that there is some specificity in the role that BRM complexes play at Notch-regulated loci.

To rule out the possibility that the effects of BrmK804R on accessibility at the *E(spl)-C* were indirect, resulting from a reduced Su(H) recruitment, we knocked down Su(H) with RNAi in the Notch-OFF condition and performed ATAC. The knockdown was effective in removing all detectable Su(H)-GFP when salivary glands were imaged live (Fig EV3D), and these conditions resulted in an increased accessibility across the *E(spl)*-C (Fig 3D). This increase in accessibility is consistent with the known role of Su(H) as a repressor of target genes in the absence of Notch signaling and contrasts with the consequences of inhibiting the BRM complex.

Together these results demonstrate that the BRM complex is necessary to maintain a degree of accessibility at enhancers, even before the cells experience Notch signaling, and is then essential for the Notch activity-dependent increase in accessibility of the *E(spl)-C*.

The BRM complex is required for acute Notch responses in Kc167 cells

To test the role of the BRM complex in a system where we could acutely manipulate Notch activity, we turned to *Drosophila* Kc167 cells. In these cells, Notch signaling is rapidly activated by the addition of the calcium chelator EGTA, which by destabilizing the negative regulatory region, elicits the rapid cleavage of the Notch receptor and activates target genes within 30 minutes [4,28,42]. As in the salivary gland, gene activation is accompanied by an increase in Su(H) recruitment, detectable by chromatin immunoprecipitation (ChIP) [4]. To test the involvement of the BRM complex in this context, we performed RNAi for two core components of the BRM complex, Brm and Snr1 (Fig 4A), and analyzed the effects on Su(H) recruitment by ChIP with qPCR. Both in Notch-OFF (Fig 4B) and Notch-ON (EGTA treatment, Fig 4C) cells, the level of Su(H) recruitment was decreased when Brm or Snr1 were depleted by RNAi, showing that the BRM complex is essential for Su(H) recruitment. The transcription of the target genes *E(spl)mβ-HLH* and *E(spl)m3-HLH,* which are usually strongly induced following Notch activation, was also decreased by *brm* RNAi (Fig 4D).

In order to confirm that the ATPase activity of the BRM complex was essential, we made stable cell lines expressing BrmK804R or the wild type form, BrmWT as a control (under control of the copper-inducible pMT promoter) [43]. Expression of *E(spl)mβ-HLH* and *E(spl)m3-HLH* was rapidly upregulated by EGTA-induced Notch activation in control conditions (Fig 4E, left). However, following copper-induced expression of BrmK804R for 24 hours, cells had a significantly reduced upregulation of *E(spl)mβ-HLH* and *E(spl)m3-HLH* compared to cells expressing BrmWT (Fig 4E, right). This shows that the ATPase function of the BRM complex is key to the Notch response in these cells.

Another sub-complex associated with SWI/SNF chromatin remodelers contains actin-related proteins (ARPs) and is proposed to facilitate sliding and ejection of nucleosomes [44–46]. To test whether this sub-complex is important for the activity of Notch-responsive enhancers, we analyzed the effects from knocking down the *Drosophila* ARP homolog, BAP55, in Kc167 cells. Strikingly, this had similar consequences to depletion of the core Brm and Snr1 subunits. Firstly, Su(H) recruitment was decreased both in Notch-OFF and Notch-ON conditions (Fig 4F), and secondly, Notch-induced RNA levels were reduced (Fig 4G). These results demonstrate an essential role for BAP55 in the Notch response and, given the data that ARPs are required for histone ejection [46], suggest that this aspect of SWI/SNF function is important mechanistically for Notch enhancer activation.

Nucleosome turnover increases with Notch signaling and is dependent on the BRM complex

Chromatin remodelers are thought to slide, replace or eject nucleosomes [13]. Even the short pulse of activity in Kc167 cells was sufficient to bring about a change in chromatin accessibility measured with ATAC (Fig EV3E), suggesting that the BRM complex could be moving or depleting histones at the Notch-regulated enhancers. Additionally, the histone variant H3.3 has been associated with nucleosome turnover [47,48]. Given the results showing changes in accessibility and histone H3.3 levels, and the involvement of BAP55, we were prompted to measure whether nucleosome turnover was occurring. To do this we used the CATCH-IT technique, which relies on the incorporation of a methionine analog called azidohomoalanine into newly-synthesized proteins [49,50]. Click chemistry is used to biotinylate this residue so that any chromatin containing newly-synthesized proteins can therefore be isolated, and a wash with high salt and urea leaves only the histone H3/H4 tetramers bound to the DNA such that histone turnover is distinguished from the incorporation of other DNA-binding proteins. We performed CATCH-IT in Kc167 cells, incubating them with media containing azidohomoalanine for four hours after a one hour period of methionine starvation, in the presence or absence of NICD. To achieve this, we used a cell line where NICD was expressed from the copper-inducible pMT promoter [4] for one hour prior to, and during both the methionine starvation and azidohomoalanine labeling. Using this approach we detected differential levels of histone turnover, with active enhancer regions showing approximately five-fold higher levels of turnover than the surrounding less active regions (Fig 5A). Notably, the enriched turnover detected at Su(H)-binding enhancer regions increased by two to three-fold in the presence of NICD.

We then tested whether knockdown of the BRM complex would affect the levels of nucleosome turnover measured with CATCH-IT. Depletion of Brm by RNAi resulted in a localized decrease in histone turnover at the Notch-responsive regions with relatively little change at control regions (Fig 5B), strengthening the evidence that the BRM complex has a critical role in Notch signaling and providing a specific mechanism by which this may occur. Furthermore, Brm depletion had an even greater effect in the Notch-ON condition when *brm* RNAi was combined with copper-inducible NICD expression (Fig 5C), illustrating the importance of the BRM complex for the Notch response.

Given that we observed increased histone H3.3 recruitment in Notch-ON cells *in vivo,* we next sought to measure the effects on the histone variant H3.3 by expressing V5-tagged histone proteins and performing ChIP [51]. When H3-V5 and H3.3-V5 were expressed from a constitutive promoter, it was evident that H3.3 predominated over H3 throughout the Notch-responsive regions of the *E(spl)*-C, while the distal region at the *E(spl)m8-HLH* gene had similar levels of both variants (Fig EV4). Neither Notch activity (Fig EV4D and E) nor depletion of Brm (Fig EV4F) had a large impact on these distributions of H3 or H3.3, arguing that there is no gross change in the overall levels of histones H3 or H3.3 during an acute Notch response, and that the BRM complex is not essential for the incorporation of H3.3 per se.

To test the dynamics of the two histone variants in this system, we then expressed H3-V5 and H3.3-V5 from the pMT promoter so that we could monitor their incorporation over a relatively short timescale. By approximately 90 minutes after their induction, the labelled histones had started to be incorporated into the chromatin (Fig EV5). By three hours after induction, differential incorporation of H3.3-V5 could be observed at specific regions, replicating the pattern seen across the *E(spl)-C* with CATCH-IT, while the levels of H3-V5 incorporation were lower and largely uniform (Fig 5D). Crucially, the incorporation of H3.3-V5 was greatly reduced following depletion of Brm, in agreement with the BRM complex having a key role in nucleosome turnover.

Discussion

In summary, we have shown that the BRM chromatin remodeling complex is essential for Notch-responsive gene activation. We propose that the BRM complex is required to maintain high levels of accessibility at Notch-responsive enhancers where it promotes rapid nucleosome turnover. Techniques that measure the nucleosome dynamics were critical in uncovering the role of the BRM complex, since the steady state levels of histones bound to the DNA do not change. Furthermore, the requirement for the ARP BAP55, whose homolog has been implicated in histone eviction [46], lends further support for our model that the BRM complex promotes nucleosome turnover. This has two implications for Notch signaling. Firstly, in the absence of Notch signaling, the BRM complex brings about local turnover of nucleosomes that enables Su(H) to access enhancers with its co-repressors, poising the enhancers for activation (Fig 6A). Secondly, BRM is responsible for the dramatic increase in chromatin accessibility at responsive genes following Notch activation (Fig 6B). It is possible that the BRM complex also plays a key role in switching off the Notch response upon cessation of signaling, since the continual turnover of nucleosomes provides a mechanism for the rapid resetting of chromatin states. In future, more fine-grained studies will be needed to determine precisely which nucleosomes are targeted by BRM complexes and what the dynamics of these interactions are.

Our evidence for the involvement of SWI/SNF chromatin remodeling in Notch signaling responses, even before signaling takes place, is fully consistent with a previous observation that BRM was recruited to Hes1 and Hes5 in mouse myoblasts before Notch induction [52]. It also fits with genetic data that hinted at a role for the BRM complex in regulating Notch target genes [22]. The fact that an antagonistic effect of Brm on Notch activity has been detected in some contexts [24] may be attributed to this role in enabling initial recruitment of CSL, as it would bring associated co-repressors [53–55]. Furthermore, since we observe consistent effects from inhibiting the BRM complex on Notch-regulated transcription in two different contexts, it is likely that the recruitment of SWI/SNF complexes will be a key step in selecting enhancer repertoires in different cell types. The SWI/SNF-dependent nucleosome turnover is therefore likely to have an integral role in generating accessible enhancer landscapes critical for the specificity of signaling pathway responses. To achieve this, BRM complexes must be recruited to target enhancers by the cell-type transcription factors that confer specificity. Candidates in the case of Notch include Runx and GATA factors which are associated with regulated enhancers in blood cell lineages (both in flies and mammals) [3,7,56,57]. Similarly, it has been suggested that the pioneer factors GATA3 and FOXA1 are required to recruit SWI/SNF complexes to enable binding of the glucocorticoid receptor at responsive sites [58].

The subsequent role of the BRM complex in bringing about a dramatic change in chromatin accessibility at responsive genes following Notch activation is critical for their up-regulation (Fig 6B). A striking feature of activated enhancers is that they exhibit a substantial increase in certain histone modifications [4,59,60], which could be facilitated by the high level of histone turnover that we detect. Indeed, a recent study has found that nucleosome

turnover is predictive of the propagation of histone modifications [61]. Furthermore, the recruitment of CSL complexes is greatly enhanced following Notch activation [6,7,62] and may be an essential step for engaging sufficient low-affinity interactions with Mediator to promote active initiation of transcription. We have previously shown that this enhanced recruitment involves changes in chromatin accessibility [8] and we now demonstrate that the BRM complex is required to enact this change. A similar model has been proposed for serum stimulation acting via FOS/JUN, where serum-induced changes in chromatin accessibility relied on BRM recruitment [17]. As several studies have shown direct interactions between NICD complexes and SWI/SNF subunits in a range of contexts [23,24,52], it is plausible that this interaction is responsible for SWI/SNF complex recruitment in Notch-ON conditions. Certainly, the BRM complex facilitates the recruitment of Su(H) in Notch-ON conditions, as evident from the depleted band of fluorescence in the presence of BrmK804R, and most likely does so by promoting nucleosome turnover. The final outcome therefore differs in in Notch-ON versus and Notch-OFF conditions, but it remains unclear how this is brought about. For example does BRM target different nucelosomes or interact with more prolonged dynamics in the Notch-ON state?

Our results argue therefore that SWI/SNF complexes are likely to play an integral role in Notch target enhancer activation. How general this effect of the BRM complex will be is an open question – to what extent is SWI/SNF remodeling critical for all types of enhancer activity? In the basal state, this complex does not appear to be required in every case, as neither heat-shock nor ecdysone-regulated loci exhibited a similar loss of accessibility when the BRM complex was perturbed. However, the mammalian SWI/SNF subunit Brg1 is required for a robust transcriptional response to glucocorticoid and was found to occupy many glucocorticoid response elements prior to hormone treatment [58]. Thus, it has been proposed that the selection and activation of hormone-responsive enhancers is reliant on the pre-patterning of specialized chromatin environments through the actions of SWI/SNF complexes in a similar manner to that proposed here. Elucidating how widely the SWI/SNF regulation of nucleosome turnover that we have detected in Notch-responsive regions underpins other classes of enhancer activation will be important, especially in the context of the frequency of mutations affecting SWI/SNF subunits in a broad spectrum of cancers.

Materials and Methods

Fly stocks

For expression of all UAS constructs in the salivary gland, 1151-Gal4 was used (L S Shashidhara, Centre for Cellular and Molecular Biology, Hyderabad, India) [63]. Notch signaling was activated by UAS-$N^{\Delta ECD}$ [30,31]. The *E(spl)-C* was imaged using the ParB-INT DNA tagging system where UAS-ParB1-mCherry was expressed in the presence of the INT sequence inserted between *E(spl)m7-HLH* and *E(spl)m8-HLH* [8,64]. Histone-GFP imaging made use of UAS-H3-GFP, UAS-H3.3-GFP and UAS-$H3.3^{core}$-GFP constructs (flies kindly provided by Kami Ahmad) [32,65]. Dynamic H3.3-mKO imaging made use of the UAS-FRT-H3.3-GFP-PolyA-FRT-H3.3-mKO-PolyA construct crossed with hs-FLP (flies kindly provided by Xin Chen) [34]. Su(H) recruitment was monitored using Su(H)-GFP [8]. Dominant negative Brm was expressed from UAS-BrmK804R [40]. RNAi lines used are listed in Table 1.

Live imaging of salivary gland nuclei

Salivary glands were dissected and mounted as described previously [8], using Shields and Sang M3 Insect Medium (Sigma S3652) supplemented with 5% FBS (Sigma F9665) and 1x Antibiotic-Antimycotic (Gibco 15240062) for dissection and the same medium with the addition of 2.5% methyl-cellulose (Sigma) for mounting. For DNA stains, salivary glands were incubated in dissecting media containing 200 µg/mL Hoechst 33342 (ThermoFisher) for 10 minutes at room temperature before washing with PBS and mounting.

Image acquisition was performed with Nikon D-Eclipse C1 confocal microscope using lasers at 405, 488 and 543 nm. Images captured of nuclei used the 60x oil objective with a 4.5x zoom level and images of glands used the 40x oil objective. To monitor Su(H)-GFP recruitment, nuclei were scanned slowly through the Z-stack using a 2x zoom level while looking for accumulations of fluorescence which were scored as bands. The scoring was not conducted blind to genotype. However, strict criteria were used to reduce subjective bias: the band of fluorescence must be bright, occupy a volume in the z-axis and most importantly, persist during microscope scanning. 10 glands and five nuclei per gland were analyzed and scored per condition, with the five nuclei closest to the coverslip chosen each time.

For dynamic H3.3-mKO imaging, heat shocks at 37°C were performed on larvae for one hour approximately 24 hours before imaging. 24 hours was chosen as a time point shortly after the mKO signal was first detectable. Image acquisition was performed with an Olympus FV1000 confocal microscope using a 60x/1.35 NA objective with spectral detectors. GFP was imaged using a laser at 488nm and subsequently mKO and mCherry were imaged simultaneously using a laser at 543nm to excite both fluorophores. The spectral detectors were set to detect wavelengths of 555 to 585 nm for mKO and 680 to 750 nm for mCherry. These wavelengths were chosen to ensure that the signal from mCherry was not observed in the mKO channel. To ensure that the two signals were fully distinguished, the

Spectral_Unmixing plugin (Joachim Walter) was used in Fiji [66] to process the images before quantification.

For quantifications of histone-GFP and mKO, representative images where the *E(spl)-C* could be clearly observed were used with the Fiji software [66] as follows. The images were rotated such that the *E(spl)-C* was vertical and a rectangle 1.29 µm by 2.58 µm was placed over it, centered on the peak fluorescence of the ParB-mCherry marker. The "plot profile" function was used to obtain mean fluorescence intensity across the rectangle in each channel. Arbitrary fluorescence values were adjusted such that the highest value obtained was set to one and the lowest to zero, and the mean values were taken from several nuclei (n numbers given in figure legend).

Immunofluorescence staining

Staining of salivary glands was performed as described [8] except for the following changes. Glands were permeabilized with 1% Triton X-100 in PBS for 30 minutes. Antibodies against OSA and BAP170 were gifts from Peter Verrijzer [67] and were used at dilutions of 1:200 and 1:100 respectively.

Kc167 cell culture, Notch activation and generation of stable lines

Kc167 cells (Drosophila Genomics Resource Center) were cultured in Schneider's *Drosophila* medium (Gibco 21720024) supplemented with 5% FBS (Sigma F9665) and 1x Antibiotic-Antimycotic (Gibco 15240062) at 25^{o}C. Notch was activated either by NICD expression from the pMT vector (cell line described below) or by EGTA treatment where media was replaced with 4 mM EGTA (Bioworld) in PBS for 30 minutes.

Stable cell lines were generated by transfection followed by antibiotic selection. 18 µg of the relevant plasmid was mixed with 925 µL Opti-MEM (Gibco 31985070) and 54 µL FuGENE HD Transfection Reagent (Promega E2311) at room temperature for 30 minutes before adding dropwise to cells plated in 10 cm plates. After 24 to 48 hours media was replaced to contain antibiotic selection. Cells were grown in the presence of antibiotic and experiments were performed after significant cell death and recovery had taken place to indicate selection (usually after approximately 3 weeks).

CATCH-IT was performed in the pMT-NICD cell line generated previously [4], where cells were maintained with 2 µg/mL puromycin (Sigma).

Cell lines expressing BrmWT and BrmK804R were generated using plasmids kindly provided by Neus Visa [43]. BrmK804R was re-made by mutagenesis to ensure homogeneity between the two constructs using Pfu polymerase with the primers listed in Table 2. The BrmWT and BrmK804R sequences were then cloned into the pMT-puro vector (Addgene 17923) by digestion with SpeI and PmeI (NEB) and ligation (T4 ligase; Promega). After transfection of pMT-BrmWT and pMT-BrmK804R, cells were selected with 5 µg/mL and maintained with 2 µg/mL puromycin.

Constitutive expression of histone-V5 proteins made use of pIB-H3-V5 and pIB-H3.3-V5 plasmids kindly provided by Dirk Schübeler and used as described [51]. Cells were selected with 50 µg/mL and maintained with 20 µg/mL blasticidin (ThermoFisher R21001). For Notch activation in these cells, they were further transfected with pMT-NICD and selected then maintained with 5 µg/mL and 2 µg/mL puromycin respectively.

For inducible expression of histone-V5 proteins, H3 and H3.3 sequences were cloned from pIB-H3-V5 and pIB-H3.3-V5 into the pMT-puro vector using SpeI and XhoI sites (NEB) with the primers listed in Table 2. After transfection of pMT-H3-V5 and pMT-H3.3-V5, cells were selected with 5 µg/mL and maintained with 2 µg/mL puromycin.

To induce expression from all pMT constructs, 5mM $CuSO_4$ was added to normal culture media. Induction was performed for 24 hours for experiments with pMT-BrmWT and pMT-BrmK804R, and for the lengths of time specified for other experiments (see CATCH-IT method for details in this experiment).

Assay for transposase-accessible chromatin

ATAC using salivary glands was performed exactly as described previously with no changes [8]. ATAC was performed in Kc167 cells in a similar manner with the following changes. After a 30-minute EGTA treatment in 10 cm culture plates containing approximately 40 million cells, cells were immediately harvested taking a quarter of the cells for the experiment (roughly 10 million). Cells were pelleted at 500xg, 4^{o}C for 5 minutes, washed in 10 mL of cold PBS and pelleted again. The cells were then lysed by resuspending in 50 µL lysis buffer (10 mM Tris-HCl, pH7.4, 10 mM NaCl, 3 mM $MgCl_2$, 0.3% NP-40), vortexing for 10 seconds, keeping on ice for 3 minutes, and vortexing again. Nuclei were pelleted at 400xg, 4^{o}C for 5 minutes and resuspended in 30 µL TD buffer (Illumina FC-121-1030). 25 µL was used for the tagmentation reaction and the rest of the protocol performed exactly as described previously for salivary glands [8].

RNAi in Kc167 cells

300 to 800 base-pair regions of *brm, Snr1* and *Bap55* DNA were amplified from genomic DNA, with *GFP* or *lacZ* sequences amplified from plasmids as controls, using either Q5 or Phusion High-Fidelity DNA Polymerases (NEB M0491 and M0530 respectively) and overhanging primers containing the T7 promoter sequence listed in Table 2. *In vitro* transcription was performed using the MEGAscript T7 Transcription Kit (Invitrogen AM1334). RNA was purified by phenol-chloroform extraction and then annealed to form double-stranded RNA by heating to 75^{o}C and cooling slowly. 100 µg double-stranded RNA was mixed with 3.5 mL Opti-MEM (Gibco 31985070) and added to approximately 10 million cells in a 10 cm plate for 30 minutes before topping up to 10 mL with normal culture medium. Volumes were scaled down for some smaller experiments.

RNA extraction and reverse transcription

To extract RNA from Kc167 cells, TRI reagent solution (Invitrogen AM6738) was used followed by phenol chloroform extraction and isopropanol precipitation at -20^{o}C overnight. For reverse transcription, RNA was resuspended in water and first DNase-treated with the DNA-free DNA Removal Kit (Invitrogen AM1906), before reverse transcribing with M-MLV Reverse Transcriptase (Promega M1705) using Oligo(dT)$_{15}$ Primers (Promega C1101). cDNA was diluted 5-fold before analysis with qPCR.

The same protocol was used to extract RNA from salivary glands, exactly as described previously [8].

Western blot

Approximately 20 million Kc167 cells were lysed in 100 µL lysis buffer (50 mM Tris-HCl, pH8.0, 150 mM NaCl, 10% glycerol, 0.5% triton X-100) on ice for 30 minutes before debris was removed by centrifugation at 13,000xg, 4^{o}C for 30 minutes. Samples were then combined with 2x loading buffer (10 mM Tris-HCl, pH6.8, 20% glycerol, 4% SDS, 0.025% bromophenol blue, 2% mercaptoethanol) and boiled. Proteins were resolved using standard protocols with 15% SDS-PAGE and transferred to nitrocellulose. Blots were probed with antibodies against histone H3 (Abcam ab1791) and V5 (Invitrogen R960-25) at dilutions of 1:1000 and 1:4000 respectively. Horseradish peroxidase-conjugated secondary antibodies were used and detected with the ECL system (GE Life Sciences).

Chromatin immunoprecipitation

Su(H) and V5 ChIP were performed largely as described previously [4,62], using 2.5 µg goat Su(H) antibody (Santa Cruz Biotechnology, no longer available) and 1-2 µg V5 antibody (Invitrogen R960-25). Briefly, cells were cross-linked with 1% formaldehyde (Sigma F8775) in PBS for 10 minutes at 25^{o}C. After lysis, chromatin was diluted 2-fold for sonication and then a further 5-fold for pre-clearing with goat or mouse IgG and 40 µL protein G or protein A/G PLUS-Agarose (Santa Cruz Biotechnology sc-2002 and sc-2003) for Su(H) and V5 ChIP respectively. Immunoprecipitation was performed with 40 µL of the same beads at 4^{o}C overnight, followed by washes, elution by vortexing, de-crosslinking with 0.3 M NaCl, 0.1 mg/mL RNase A and 0.1 mg/mL proteinase K treatment. DNA was purified with the QIAquick PCR purification kit (Qiagen) and eluted in 100 µL water for analysis with qPCR.

CATCH-IT

Schneider's Drosophila medium without methionine (PAN Biotech), supplemented with 5% FBS and 1x Antibiotic-Antimycotic was added to cells for 1 hour, followed by adding either 4 mM azidohomoalanine (Aha; AnaSpec AS-63669) or 4 mM methionine (Sigma) as a control for 4 hours. To activate Notch, pMT-NICD cells were induced with 5 mM $CuSO_4$ for 1 hour

before the medium was substituted for methionine-free medium, also containing 5 mM $CuSO_4$, so that cells were incubated with $CuSO_4$ for a total of 6 hours.

CATCH-IT was performed as previously described [50], except where stated otherwise. Briefly, cells were harvested and nuclei were extracted with 30 µL of 10% NP-40. Nuclei were resuspended in 180 µL of HB125 buffer, and the following were added: 5 µL of 2 nM biotin-alkyne (Invitrogen B10185), 10 µL of 100mM THPTA (Sigma 762342) premixed with 2 µL of 100 mM copper sulfate (Jena Bioscience CLK-M1004), and 6 µL of freshly-prepared 500 mM sodium ascorbate (Jena Bioscience CLK-M1005). Cycloaddition reaction was performed for 30 minutes at room temperature on a rotor. Reaction with MNase (Sigma N3755) was performed at 37°C for 3 minutes. After capture with Dynabeads M-280 Streptavidin (Invitrogen 11205) as described, captured chromatin and input chromatin samples were treated with 0.25 mg/mL RNase A (Roche) and 0.25 mg/mL proteinase K (ThermoFisher). DNA was purified with the QIAquick PCR purification kit (Qiagen) and analyzed by qPCR.

qPCR

All qPCR was performed using LightCycler 480 SYBR Green I Mastermix (Roche 04707516001) as described previously [8]. For all experiments, two technical replicate qPCR reactions were performed per sample and the mean taken for analysis. Replicate numbers given in figure legends do not count these technical replicates and instead refer only to repeats of the full experimental protocol from start to finish with different cells or animals (biological replicates). For reverse transcription experiments, relative amounts of the genes of interest were normalized to the control gene RpL32. For ChIP, immunoprecipitated samples were normalized to input samples. For CATCH-IT, pulldown samples were normalized to input samples and then to the Sec15 transcribed region. All primers used are shown in Table 2.

Tables

Table 1 - RNAi lines used.

RNAi	Source[1]	Phenotype shown in published work
w	BL-35573	Used as a control in [8,68]
Iswi	BL-32845	[69]
Chrac-16	BL-51155	[69]
MTA1-like	BL-33745	[68]
Ino80	BL-33708	[70]
Tip60	BL-28563	[71]
Chd1	BL-34665	[70]
Chd3	V-13636	Not used previously
Snr1	BL-32372	[72]
Moira	BL-34919	[73]
osa (1)	BL-31266	[74]
osa (2)	V-7810	[75]
Bap170	BL-26308	[76]
polybromo	BL-32840	[76]
Caf1-55	V-26455	[77] (same construct used, inserted in a different chromosome)
Caf1-180	BL-28918	[77]
Dek	BL-28696	Not used previously
yem	V-26808	[78]
zeste	BL-31615	Not used previously

[1] Bloomington *Drosophila* Stock Center is abbreviated BL, and Vienna *Drosophila* RNAi Centre is abbreviated V.

Table 2 - All primers used.

Name	Sequence
BrmK804R mutagenesis	
K804R_forward	CCGATGAAATGGGTTTGGGTCGAACCATTCAAACCATTTCGC
K804R_reverse	GCGAAATGGTTTGAATGGTTCGACCCAAACCCATTTCATCGG
Histone-V5 cloning into pMT vector	
SpeI_his_forward	CCTACTAGTCATGGCTCGTACCAAGCAAACTGC
XhoI_his_reverse	CACCTCGAGGCGGCCGCCACTGTGCTGGATA
T7 primers for making double-stranded RNA	
T7_GFP_forward	TAGTAATACGACTCACTATAGGGAAAGGGCAGATTGTGTGGAC
T7_GFP_reverse	TAGTAATACGACTCACTATAGGGTCAAGGACGACGGGAACTAC
T7_LacZ_forward	CCGAATTAATACGACTCACTATAGGGCCGCTGGATAACGACATTGG
T7_LacZ_reverse	CCGAATTAATACGACTCACTATAGGGGACTGTAGCGGCTGATGTTG
T7_Brm_forward	TAGTAATACGACTCACTATAGGGCGATCATAAACCCAAGGTGG
T7_Brm_reverse	TAGTAATACGACTCACTATAGGGCAGTGATGGTTCTTCATGCG
T7_Snr1_forward	TAGTAATACGACTCACTATAGGGCTGGACATGGAGCTAGAGGG

T7_Snr1_reverse	TAGTAATACGACTCACTATAGGGCGTCGGTAAGCGTCTCTAGG
T7_Bap55_forward	TAGTAATACGACTCACTATAGGGACGGCATGATTGACAACTGG
T7_Bap55_reverse	TAGTAATACGACTCACTATAGGGTGCCACGACTGAGTTAGGTT
qPCR: E(spl)-C	
mγ-mβ igr_forward	GGAGTTGAGGAGTTGGTCG
mγ-mβ igr_reverse	ATAAGTGTGGTTGGGTGCCT
mβ tr_forward	AGAAGTGAGCAGCAGCCATC
mβ tr_reverse	GCTGGACTTGAAACCGCACC
mβ enh_forward	AGAGGTCTGTGCGACTTGG
mβ enh_reverse	GGATGGAAGGCATGTGCT
mβ-mα igr_forward	AAGCCAGTGGACTCTGCTCT
mβ-mα igr_reverse	TGATCTCCAAGCGGAGTATG
mα tr_forward	GCAGGAGGACGAGGAGGATG
mα tr_reverse	GATCCTGGAATTGCATGGAG
m2-m3 igr_forward	GCGCGTATTTCCCAAATAAA
m2-m3 igr_reverse	GATTGTACGTGCATGGGAAA
m3 enh_forward	ACACACACAAACACCCATCC
m3 enh_reverse	CGAGGCAGTAGCCTATGTGA
m3 tr_forward	CGTCTGCAGCTCAATTAGTC
m3 tr_reverse	AGCCCACCCACCTCAACCAG
m8 tr_forward	CAATTCCACGAAGCACAGTC
m8 tr_reverse	GAGGAGCAGTCCATCGAGTT
qPCR: additional controls for ATAC	
Rab11 tr_forward	ACTGAAAATGGGCCGTTTCG
Rab11 tr_reverse	AGGAGTGGTAATCGACGGTC
Eip78C enh_forward	AGAAGTAGGGGCCGTCAAGT
Eip78C enh_reverse	GTGTAAGACCCGTCGCATTT
Closed ctrl_forward	GCATTTTTGTGGCAGAGGCA
Closed ctrl_reverse	CTCTTTCGGTGTCGCCTTCT
Mst87F tr_forward	ATCCTTTGCCTCTTCAGTCC
Mst87F tr_reverse	AATAATGATACAAAATCTGGTTACGC
Hsp26 tr_forward	TTGAATTCGATCTGTGCTCTGT
Hsp26 tr_reverse	CGGGTATAAAAGCAGCGTCG
Hsp70 enh_forward	TCGTTTTGTGACTCTCCCTCT
Hsp70 enh_reverse	TGTGACAGAGTGAGAGAGCA
Hr4 enh_forward	GGCACCTGACGGTTGATAGT
Hr4 enh_reverse	CAGCCCGAAGAATCTACCAG
Dip-B tr_forward	TCAACTGCAACCGGATGATA
Dip-B tr_reverse	ATAACCTCATCGGCCACGTA
Eip75B tr_forward	AGCAACTTGGCCAGGAACT
Eip75B tr_reverse	AACCTGGAGCTGATCGAGAA
CTPsyn tr_forward	TCGATTGTTGTTGGCTGAGC
CTPsyn tr_reverse	TTCCTTCGCTCTTCCTGTCC
fru tr_forward	CTCTTTCGCACACTTGGCAT
fru tr_reverse	CCGTTCGTTGCCCATCTAAG
kay tr_forward	CTCTCTCATTGGCTCTCCCC

kay tr_reverse	TGAAGCGGAGACCACACAAT
vri tr_forward	TGTGTGTTTGTGTCTGCGAG
vri tr_reverse	TCACTCACCCTCACCATGAC
qPCR: additional controls for RT-qPCR	
RpL32_forward	ACGTTGTGCACCAGGAACTT
RpL32_reverse	CCGCTTCAAGGGACAGTATC
RpII215_forward	GACTCGACTGGAATTGCACC
RpII215_reverse	TCTTCATCGGGATACTCGCC
qPCR: additional controls for CATCH-IT	
PPO1 enh_forward	AAGTCCCAACCGCAAAACTG
PPO1 enh_reverse	GCTATCGACTAAACCACAACGT
Him-Her enh_forward	CGAACCGAGTTGTGGGAAAT
Him-Her enh_reverse	CCCTTGGAGTGACAATTAGCTG
Rab11 tr_forward	ACTGAAAATGGGCCGTTTCG
Rab11 tr_reverse	AGGAGTGGTAATCGACGGTC
Sec15 tr_forward	GGTAGCGGTTCTCTTGCTTG
Sec15 tr_reverse	GTAACCGTCAGCTGTTGGAC

Acknowledgements

We thank Jin Li, Damiano Porcelli and members of the Bray Lab for technical advice and helpful discussions. This work was supported by a Programme Grant from the Medical Research Council to SJB (MR/L007177/1) and by a studentship from BBSRC for ZP (1502069).

Author Contributions

SJB and ZP conceived the project, SJB supervised the work, ZP performed the experiments and analyzed the data, ZP and SJB wrote the manuscript.

Conflict of Interest

The authors declare no conflicts of interest.

References

1. Penton AL, Leonard LD, Spinner NB (2012) Notch signaling in human development and disease. *Semin Cell Dev Biol* **23**: 450–457.

2. Bray SJ (2016) Notch signalling in context. *Nat Rev Mol Cell Biol* **17**: 722–735.

3. Terriente-Felix A, Li J, Collins S, Mulligan A, Reekie I, Bernard F, Krejci A, Bray S (2013) Notch cooperates with Lozenge/Runx to lock haemocytes into a differentiation programme. *Development* **140**: 926–937.

4. Skalska L, Stojnic R, Li J, Fischer B, Cerda-Moya G, Sakai H, Tajbakhsh S, Russell S, Adryan B, Bray SJ (2015) Chromatin signatures at Notch-regulated enhancers reveal large-scale changes in H3K56ac upon activation. *EMBO J* **34**: 1889–1904.

5. Bray SJ, Gomez-Lamarca M (2018) Notch after cleavage. *Curr Opin Cell Biol* **51**: 103–109.

6. Castel D, Mourikis P, Bartels SJJ, Brinkman AB, Tajbakhsh S, Stunnenberg HG (2013) Dynamic binding of RBPJ is determined by Notch signaling status. *Genes Dev* **27**: 1059–1071.

7. Wang H, Zang C, Taing L, Arnett KL, Wong YJ, Pear WS, Blacklow SC, Liu XS, Aster JC (2014) NOTCH1-RBPJ complexes drive target gene expression through dynamic interactions with superenhancers. *Proc Natl Acad Sci* **111**: 705–710.

8. Gomez-Lamarca MJ, Falo-Sanjuan J, Stojnic R, Abdul Rehman S, Muresan L, Jones ML, Pillidge Z, Cerda-Moya G, Yuan Z, Baloul S, et al. (2018) Activation of the Notch Signaling Pathway In Vivo Elicits Changes in CSL Nuclear Dynamics. *Dev Cell* **44**: 611–623.e7.

9. Oswald F, Rodriguez P, Giaimo BD, Antonello ZA, Mira L, Mittler G, Thiel VN, Collins KJ, Tabaja N, Cizelsky W, et al. (2016) A phospho-dependent mechanism involving NCoR and KMT2D controls a permissive chromatin state at Notch target genes. *Nucleic Acids Res* **44**: 4703–4720.

10. Giaimo BD, Ferrante F, Vallejo DM, Hein K, Gutierrez-Perez I, Nist A, Stiewe T, Mittler G, Herold S, Zimmermann T, et al. (2018) Histone variant H2A.Z deposition and acetylation directs the canonical Notch signaling response. *Nucleic Acids Res*.

11. Nair SS, Kumar R (2012) Chromatin remodeling in cancer: a gateway to regulate gene transcription. *Mol Oncol* **6**: 611–619.

12. Venkatesh S, Workman JL (2015) Histone exchange, chromatin structure and the regulation of transcription. *Nat Rev Mol Cell Biol* **16**: 178–189.

13. Längst G, Manelyte L (2015) Chromatin Remodelers: From Function to Dysfunction. *Genes (Basel)* **6**: 299–324.

14. Clapier CR, Iwasa J, Cairns BR, Peterson CL (2017) Mechanisms of action and regulation of ATP-dependent chromatin-remodelling complexes. *Nat Rev Mol Cell Biol* **18**: 407–422.

15. Wang L, Du Y, Ward JM, Shimbo T, Lackford B, Zheng X, Miao Y, Zhou B, Han L, Fargo

DC, et al. (2014) INO80 Facilitates Pluripotency Gene Activation in Embryonic Stem Cell Self-Renewal, Reprogramming, and Blastocyst Development. *Cell Stem Cell* **14**: 575–591.

16. Zhou B, Wang L, Zhang S, Bennett BD, He F, Zhang Y, Xiong C, Han L, Diao L, Li P, et al. (2016) INO80 governs superenhancer-mediated oncogenic transcription and tumor growth in melanoma. *Genes Dev* **30**: 1440–1453.

17. Vierbuchen T, Ling E, Cowley CJ, Couch CH, Wang X, Harmin DA, Roberts CWM, Greenberg ME (2017) AP-1 Transcription Factors and the BAF Complex Mediate Signal-Dependent Enhancer Selection. *Mol Cell* **68**: 1067–1082.e12.

18. Hu G, Schones DE, Cui K, Ybarra R, Northrup D, Tang Q, Gattinoni L, Restifo NP, Huang S, Zhao K (2011) Regulation of nucleosome landscape and transcription factor targeting at tissue-specific enhancers by BRG1. *Genome Res* **21**: 1650–1658.

19. Fryer CJ, Archer TK (1998) Chromatin remodelling by the glucocorticoid receptor requires the BRG1 complex. *Nature* **393**: 88–91.

20. Nagaich AK, Walker DA, Wolford R, Hager GL (2004) Rapid periodic binding and displacement of the glucocorticoid receptor during chromatin remodeling. *Mol Cell* **14**: 163–174.

21. Kadoch C, Crabtree GR (2015) Mammalian SWI/SNF chromatin remodeling complexes and cancer: Mechanistic insights gained from human genomics. *Sci Adv* **1**: e1500447–e1500447.

22. Armstrong JA, Sperling AS, Deuring R, Manning L, Moseley SL, Papoulas O, Piatek CI, Doe CQ, Tamkun JW (2005) Genetic Screens for Enhancers of brahma Reveal Functional Interactions Between the BRM Chromatin-Remodeling Complex and the Delta-Notch Signal Transduction Pathway in Drosophila. *Genetics* **170**: 1761–1774.

23. Takeuchi JK, Lickert H, Bisgrove BW, Sun X, Yamamoto M, Chawengsaksophak K, Hamada H, Yost HJ, Rossant J, Bruneau BG (2007) Baf60c is a nuclear Notch signaling component required for the establishment of left–right asymmetry. *Proc Natl Acad Sci* **104**: 846–851.

24. Das A V, James J, Bhattacharya S, Imbalzano AN, Antony ML, Hegde G, Zhao X, Mallya K, Ahmad F, Knudsen E, et al. (2007) SWI/SNF chromatin remodeling ATPase Brm regulates the differentiation of early retinal stem cells/progenitors by influencing Brn3b expression and Notch signaling. *J Biol Chem* **282**: 35187–35201.

25. Xie G, Chen H, Jia D, Shu Z, Palmer WH, Huang Y-C, Zeng X, Hou SX, Jiao R, Deng W-M (2017) The SWI/SNF Complex Protein Snr1 Is a Tumor Suppressor in Drosophila Imaginal Tissues. *Cancer Res* **77**: 862–873.

26. Bailey AM, Posakony JW (1995) Suppressor of hairless directly activates transcription of enhancer of split complex genes in response to Notch receptor activity. *Genes Dev* **9**: 2609–2622.

27. Cooper MTD, Tyler DM, Furriols M, Chalkiadaki A, Delidakis C, Bray S (2000) Spatially Restricted Factors Cooperate with Notch in the Regulation of Enhancer of split Genes. *Dev Biol* **221**: 390–403.

28. Housden BE, Fu AQ, Krejci A, Bernard F, Fischer B, Tavaré S, Russell S, Bray SJ (2013) Transcriptional Dynamics Elicited by a Short Pulse of Notch Activation Involves Feed-Forward Regulation by E(spl)/Hes Genes. *PLoS Genet* **9**: e1003162.

29. Schaaf CA, Misulovin Z, Gause M, Koenig A, Dorsett D (2013) The Drosophila enhancer of split gene complex: architecture and coordinate regulation by notch, cohesin, and polycomb group proteins. *G3 (Bethesda)* **3**: 1785–1794.

30. Fortini ME, Rebay I, Caron LA, Artavanis-Tsakonas S (1993) An activated Notch receptor blocks cell-fate commitment in the developing Drosophila eye. *Nature* **365**: 555–557.

31. Rebay I, Fehon RG, Artavanis-Tsakonas S (1993) Specific truncations of Drosophila Notch define dominant activated and dominant negative forms of the receptor. *Cell* **74**: 319–329.

32. Ahmad K, Henikoff S (2002) The Histone Variant H3.3 Marks Active Chromatin by Replication-Independent Nucleosome Assembly. *Mol Cell* **9**: 1191–1200.

33. Mito Y, Henikoff JG, Henikoff S (2005) Genome-scale profiling of histone H3.3 replacement patterns. *Nat Genet* **37**: 1090–1097.

34. Tran V, Lim C, Xie J, Chen X (2012) Asymmetric division of Drosophila male germline stem cell shows asymmetric histone distribution. *Science* **338**: 679–682.

35. Bouazoune K, Brehm A (2006) ATP-dependent chromatin remodeling complexes in Drosophila. *Chromosom Res* **14**: 433–449.

36. Sawatsubashi S, Murata T, Lim J, Fujiki R, Ito S, Suzuki E, Tanabe M, Zhao Y, Kimura S, Fujiyama S, et al. (2010) A histone chaperone, DEK, transcriptionally coactivates a nuclear receptor. *Genes Dev* **24**: 159–170.

37. Orsi GA, Algazeery A, Meyer RE, Capri M, Sapey-Triomphe LM, Horard B, Gruffat H, Couble P, Aït-Ahmed O, Loppin B (2013) Drosophila Yemanuclein and HIRA cooperate for de novo assembly of H3.3-containing nucleosomes in the male pronucleus. *PLoS Genet* **9**: e1003285.

38. Mohrmann L, Verrijzer CP (2005) Composition and functional specificity of SWI2/SNF2 class chromatin remodeling complexes. *Biochim Biophys Acta - Gene Struct Expr* **1681**: 59–73.

39. Hodges C, Kirkland JG, Crabtree GR (2016) The Many Roles of BAF (mSWI/SNF) and PBAF Complexes in Cancer. *Cold Spring Harb Perspect Med* **6**:.

40. Elfring LK, Daniel C, Papoulas O, Deuring R, Sarte M, Moseley S, Beek SJ, Waldrip WR, Daubresse G, DePace A, et al. (1998) Genetic analysis of brahma: the Drosophila homolog of the yeast chromatin remodeling factor SWI2/SNF2. *Genetics* **148**: 251–265.

41. Buenrostro JD, Wu B, Chang HY, Greenleaf WJ (2015) ATAC-seq: A Method for Assaying Chromatin Accessibility Genome-Wide. In, *Current Protocols in Molecular Biology* p 21.29.1-21.29.9. John Wiley & Sons, Inc., Hoboken, NJ, USA.

42. Rand MD, Grimm LM, Artavanis-Tsakonas S, Patriub V, Blacklow SC, Sklar J, Aster JC (2000) Calcium depletion dissociates and activates heterodimeric notch receptors. *Mol Cell Biol* **20**: 1825–1835.

43. Yu S, Waldholm J, Böhm S, Visa N (2014) Brahma regulates a specific trans-splicing event at the mod(mdg4) locus of Drosophila melanogaster. *RNA Biol* **11**: 134–145.

44. Cairns BR, Erdjument-Bromage H, Tempst P, Winston F, Kornberg RD (1998) Two actin-related proteins are shared functional components of the chromatin-remodeling complexes RSC and SWI/SNF. *Mol Cell* **2**: 639–651.

45. Schubert HL, Wittmeyer J, Kasten MM, Hinata K, Rawling DC, Héroux A, Cairns BR, Hill CP (2013) Structure of an actin-related subcomplex of the SWI/SNF chromatin remodeler. *Proc Natl Acad Sci* **110**: 3345–3350.

46. Clapier CR, Kasten MM, Parnell TJ, Viswanathan R, Szerlong H, Sirinakis G, Zhang Y, Cairns BR (2016) Regulation of DNA Translocation Efficiency within the Chromatin Remodeler RSC/Sth1 Potentiates Nucleosome Sliding and Ejection. *Mol Cell* **62**: 453–461.

47. Huang C, Zhu B (2014) H3.3 turnover: a mechanism to poise chromatin for transcription, or a response to open chromatin? *Bioessays* **36**: 579–584.

48. Deaton AM, Gómez-Rodríguez M, Mieczkowski J, Tolstorukov MY, Kundu S, Sadreyev RI, Jansen LE, Kingston RE (2016) Enhancer regions show high histone H3.3 turnover that changes during differentiation. *Elife* **5**:.

49. Deal RB, Henikoff JG, Henikoff S (2010) Genome-Wide Kinetics of Nucleosome Turnover Determined by Metabolic Labeling of Histones. *Science (80-)* **328**: 1161–1164.

50. Teves SS, Deal RB, Henikoff S (2012) Measuring genome-wide nucleosome turnover using CATCH-IT. *Methods Enzymol* **513**: 169–184.

51. Wirbelauer C, Bell O, Schübeler D (2005) Variant histone H3.3 is deposited at sites of nucleosomal displacement throughout transcribed genes while active histone modifications show a promoter-proximal bias. *Genes Dev* **19**: 1761–1766.

52. Kadam S, Emerson BM (2003) Transcriptional Specificity of Human SWI/SNF BRG1 and BRM Chromatin Remodeling Complexes. *Mol Cell* **11**: 377–389.

53. Kao HY, Ordentlich P, Koyano-Nakagawa N, Tang Z, Downes M, Kintner CR, Evans RM, Kadesch T (1998) A histone deacetylase corepressor complex regulates the Notch signal transduction pathway. *Genes Dev* **12**: 2269–2277.

54. Hsieh JJ, Zhou S, Chen L, Young DB, Hayward SD (1999) CIR, a corepressor linking the DNA binding factor CBF1 to the histone deacetylase complex. *Proc Natl Acad Sci U S A* **96**: 23–28.

55. Collins KJ, Yuan Z, Kovall RA (2014) Structure and function of the CSL-KyoT2 corepressor complex: a negative regulator of Notch signaling. *Structure* **22**: 70–81.

56. Muratoglu S, Hough B, Mon ST, Fossett N (2007) The GATA factor Serpent cross-

regulates lozenge and u-shaped expression during Drosophila blood cell development. *Dev Biol* **311**: 636–649.

57. Mehta C, Johnson KD, Gao X, Ong IM, Katsumura KR, McIver SC, Ranheim EA, Bresnick EH (2017) Integrating Enhancer Mechanisms to Establish a Hierarchical Blood Development Program. *Cell Rep* **20**: 2966–2979.

58. Hoffman JA, Trotter KW, Ward JM, Archer TK (2018) BRG1 governs glucocorticoid receptor interactions with chromatin and pioneer factors across the genome. *Elife* **7**:.

59. Mikkelsen TS, Ku M, Jaffe DB, Issac B, Lieberman E, Giannoukos G, Alvarez P, Brockman W, Kim T-K, Koche RP, et al. (2007) Genome-wide maps of chromatin state in pluripotent and lineage-committed cells. *Nature* **448**: 553–560.

60. Creyghton MP, Cheng AW, Welstead GG, Kooistra T, Carey BW, Steine EJ, Hanna J, Lodato MA, Frampton GM, Sharp PA, et al. (2010) Histone H3K27ac separates active from poised enhancers and predicts developmental state. *Proc Natl Acad Sci U S A* **107**: 21931–21936.

61. Chory EJ, Calarco JP, Hathaway NA, Bell O, Neel DS, Crabtree GR (2019) Nucleosome Turnover Regulates Histone Methylation Patterns over the Genome. *Mol Cell* **73**: 61–72.e3.

62. Krejci A, Bray S (2007) Notch activation stimulates transient and selective binding of Su(H)/CSL to target enhancers. *Genes Dev* **21**: 1322–1327.

63. Roy S, VijayRaghavan K (1997) Homeotic genes and the regulation of myoblast migration, fusion, and fibre-specific gene expression during adult myogenesis in Drosophila. *Development* **124**: 3333–3341.

64. Saad H, Gallardo F, Dalvai M, Tanguy-le-Gac N, Lane D, Bystricky K (2014) DNA dynamics during early double-strand break processing revealed by non-intrusive imaging of living cells. *PLoS Genet* **10**: e1004187.

65. Henikoff S, Ahmad K, Platero JS, van Steensel B (2000) Heterochromatic deposition of centromeric histone H3-like proteins. *Proc Natl Acad Sci U S A* **97**: 716–721.

66. Schindelin J, Arganda-Carreras I, Frise E, Kaynig V, Longair M, Pietzsch T, Preibisch S, Rueden C, Saalfeld S, Schmid B, et al. (2012) Fiji: an open-source platform for biological-image analysis. *Nat Methods* **9**: 676–682.

67. Moshkin YM, Mohrmann L, van Ijcken WFJ, Verrijzer CP (2007) Functional differentiation of SWI/SNF remodelers in transcription and cell cycle control. *Mol Cell Biol* **27**: 651–661.

68. Nikalayevich E, Ohkura H (2015) The NuRD nucleosome remodelling complex and NHK-1 kinase are required for chromosome condensation in oocytes. *J Cell Sci* **128**: 566–575.

69. Börner K, Jain D, Vazquez-Pianzola P, Vengadasalam S, Steffen N, Fyodorov D V, Tomancak P, Konev A, Suter B, Becker PB (2016) A role for tuned levels of nucleosome remodeler subunit ACF1 during Drosophila oogenesis. *Dev Biol* **411**: 217–230.

70. Ellis K, Friedman C, Yedvobnick B (2015) Drosophila domino Exhibits Genetic Interactions with a Wide Spectrum of Chromatin Protein-Encoding Loci. *PLoS One* **10**: e0142635.

71. Kwon MH, Callaway H, Zhong J, Yedvobnick B (2013) A targeted genetic modifier screen links the SWI2/SNF2 protein domino to growth and autophagy genes in Drosophila melanogaster. *G3 (Bethesda)* **3**: 815–825.

72. Berson A, Sartoris A, Nativio R, Van Deerlin V, Toledo JB, Porta S, Liu S, Chung C-Y, Garcia BA, Lee VM-Y, et al. (2017) TDP-43 Promotes Neurodegeneration by Impairing Chromatin Remodeling. *Curr Biol* **27**: 3579–3590.e6.

73. Oh H, Slattery M, Ma L, Crofts A, White KP, Mann RS, Irvine KD (2013) Genome-wide Association of Yorkie with Chromatin and Chromatin-Remodeling Complexes. *Cell Rep* **3**: 309–318.

74. Anderson AE, Galko MJ (2014) Rapid clearance of epigenetic protein reporters from wound edge cells in Drosophila larvae does not depend on the JNK or PDGFR/VEGFR signaling pathways. *Regen (Oxford, England)* **1**: 11–25.

75. Zeng X, Lin X, Hou SX (2013) The Osa-containing SWI/SNF chromatin-remodeling complex regulates stem cell commitment in the adult Drosophila intestine. *Development* **140**: 3532–3540.

76. He J, Xuan T, Xin T, An H, Wang J, Zhao G, Li M (2014) Evidence for Chromatin-Remodeling Complex PBAP-Controlled Maintenance of the Drosophila Ovarian Germline Stem Cells. *PLoS One* **9**: e103473.

77. Yu Z, Wu H, Chen H, Wang R, Liang X, Liu J, Li C, Deng W-M, Jiao R (2013) CAF-1 promotes Notch signaling through epigenetic control of target gene expression during Drosophila development. *Development* **140**: 3635–3644.

78. Chen W-Y, Shih H-T, Liu K-Y, Shih Z-S, Chen L-K, Tsai T-H, Chen M-J, Liu H, Tan BC-M, Chen C-Y, et al. (2015) Intellectual disability-associated dBRWD3 regulates gene expression through inhibition of HIRA/YEM-mediated chromatin deposition of histone H3.3. *EMBO Rep* **16**: 528–538.

Figure Legends

Figure 1 - H3.3 levels increase at the *E(spl)-C* in Notch-ON nuclei.

A, C, E Live imaging of histone-GFP (green) and ParB-mCherry (magenta) expressed in larval salivary gland nuclei using 1151-Gal4. H3.3-GFP levels are increased at the *E(spl)-C* in the presence of constitutively active Notch, $N^{\Delta ECD}$ (Notch-ON), compared to control Notch-OFF nuclei expressing LacZ (A). The same is seen with $H3.3^{core}$-GFP (E), but there is little change in H3-GFP between Notch-OFF and Notch-ON nuclei (C). ParB-mCherry binds to its cognate *int* DNA sequence inserted within the *E(spl)-C* [8,64]. Yellow dotted box contains *E(spl)-C* and yellow arrow indicates position of *E(spl)-C* on chromosome. Scale bars (white) = 5 µm.

B, D, F Quantifications of relative fluorescence intensity of histone-GFP and ParB-mCherry across the *E(spl)-C* in Notch-OFF (upper) and Notch-ON (lower) conditions. Mean+/-SEM; n_{nuclei} = 7, 6, 5, 8, 9, 11 and n_{glands} = 5, 5, 5, 5, 5, 4 where each gland represents a biological replicate (from top to bottom).

Figure 2 - The BRM complex is required for Su(H) recruitment in Notch-ON nuclei.

A, C Effects from depleting chromatin remodelers and histone chaperones, as indicated (wide range shown in A, BRM complex components shown in C), on recruitment of Su(H)-GFP in Notch-ON nuclei (expressing $N^{\Delta ECD}$) of larval salivary glands. *w* RNAi is a control and BrmK804R is expression of dominant-negative Brm. Different *OSA* RNAi stocks used in C are denoted by (1) and (2). In all conditions except *Moira* RNAi (A), *Snr1* RNAi and BrmK804R expression (C), nuclei exhibit a bright accumulation of Su(H)-GFP at a single locus when imaged live. Scale bars (yellow) = 5 µm.

B, D Percentage of Notch-ON nuclei retaining a single clear band of Su(H)-GFP when the indicated RNAi is co-expressed with $N^{\Delta ECD}$. For each genotype, 5 nuclei from each of 10 glands were scored (50 nuclei total). **** A significant fraction of nuclei lost the fluorescent band when core components of the BRM complex were perturbed; $p<0.0001$, two-tailed Fisher's exact test calculated using the raw (non-percentage) scoring data.

Figure 3 - The BRM complex is required for chromatin accessibility at Notch-responsive regions.

A Genomic region encompassing the *E(spl)-C*; green graphs indicate ChIP enrichment for Su(H) in Kc167 cells (Log_2 scale is -0.5 to 2.9, data published previously in [4]); gene models are depicted in dark blue. Positions of primer pairs used in qPCR experiments are indicated with black arrows. Abbreviations are as follows: "igr" = intergenic region, "tr" = transcribed region and "enh" = enhancer.

B, C Chromatin accessibility in Notch-OFF (B) and Notch-ON ($N^{\Delta ECD}$ expression, C) salivary gland nuclei measured by ATAC-qPCR; fold enrichment at the indicated regions compared to

a “closed ctrl” region. Expression of dominant-negative Brm, BrmK804R, led to reduced accessibility of *E(spl)mβ-HLH* and *E(spl)m3-HLH* enhancer regions in Notch-OFF conditions, and to a more widespread reduction in accessibility in Notch-ON conditions. “Eip78C enh” corresponds to the ecdysone receptor-binding region of the Eip78C enhancer, which is highly accessible but not Notch-responsive; “Rab11 tr” and “Mst87F tr” represent highly and lowly-expressed control genes respectively. Mean +/- SEM; n = 3; * $p<0.05$ with two-tailed Welch’s t-test comparing LacZ and BrmK804R samples.

D Chromatin accessibility in salivary gland nuclei depleted for Su(H) by RNAi, measured by ATAC-qPCR; fold enrichment at the indicated regions compared to a “closed ctrl” region. Accessibility is increased across most of the *E(spl)-C* compared to controls expressing LacZ. Control primer regions are as in B and C. Mean +/- SEM; n = 3; * $p<0.05$ with two-tailed Welch’s t-test compared to LacZ controls.

Figure 4 - The BRM complex is required for Su(H) recruitment and Notch-dependent transcription in Kc167 cells.

A Effect of *brm* and *Snr1* RNAi on *brm* and *Snr1* cDNA levels respectively, measured by reverse transcription-qPCR in Kc167 cells; percentage cDNA compared to *GFP* RNAi. The knockdowns are highly effective, with only 1-2% of *brm* and *Snr1* cDNA remaining detectable. Mean +/- SEM; n = 3.

B, C Knockdown of components of the BRM complex reduces Su(H) recruitment both in Notch-OFF (B) and Notch-ON (C) conditions. Fold enrichment of Su(H) occupancy at the indicated positions detected by ChIP, relative to input, in Kc167 cells treated with *brm*, *Snr1* or *GFP* RNAi as a control. Notch-ON conditions (C) were induced by 30 minutes of EGTA treatment. Mean +/- SEM, n = 3 (B); Mean, n = 2 (C); * $p<0.05$ with one-tailed student’s t-test compared to *GFP* RNAi control.

D Effect of *brm* RNAi on *E(spl)mβ-HLH* (mβ) and *E(spl)m3-HLH* (m3) induction by Notch activation (EGTA treatment) measured by reverse transcription-qPCR; shown as fold difference to *lacZ* RNAi control. Mean +/- SEM; n = 3.

E Effect of Brm dominant-negative on expression of *E(spl)mβ-HLH* (mβ) and *E(spl)m3-HLH* (m3) measured by reverse transcription-qPCR. Expression was analyzed in stable cell lines containing pMT-inducible BrmWT or BrmK804R in the absence (left, uninduced) or presence of copper sulfate (right, Cu^{2+} induced). The response of *E(spl)mβ-HLH* and *E(spl)m3-HLH* to Notch activation (“N-On” = EGTA treatment vs. “N-Off” = PBS control) was reduced in the BrmK804R-expressing cells compared to BrmWT-expressing cells, only when induced with copper (right graph). Mean, n = 2 (left); Mean +/- SEM, n = 3 (right); * $p<0.05$ with one-tailed student’s t-test comparing BrmWT and BrmK804R.

F Knockdown of actin-related subunit, BAP55, reduces Su(H) recruitment in both Notch-OFF (PBS treatment) and Notch-ON (EGTA treatment) conditions. Fold enrichment of Su(H) occupancy at the indicated positions detected by ChIP, relative to input, in Kc167 cells

treated with *Bap55* or *lacZ* RNAi as a control. Mean +/- SEM; n = 3; * p<0.05 with one-tailed student's t-test compared to *lacZ* RNAi control.

G Effect of *Bap55* RNAi on *E(spl)mβ-HLH* (mβ) and *E(spl)m3-HLH* (m3) expression levels measured by reverse transcription-qPCR in Notch-OFF (PBS treatment) and Notch-ON (EGTA treatment) conditions. Expression level of *RpII215* is shown as a control gene. Mean +/- SEM; n = 3; * p<0.05 with one-tailed student's t-test compared to *lacZ* RNAi control.

Figure 5 - Nucleosome turnover at Su(H)-bound enhancers is increased in Notch-ON cells and is dependent on the BRM complex.

A Nucleosome turnover measured by CATCH-IT-qPCR; fold enrichment over input samples compared to Sec15 tr control region. Su(H)-bound enhancers show increased nucleosome turnover in response to Notch signaling. Notch signaling is activated in Kc167 cells by 6 hours of copper induction of pMT-NICD with copper excluded in the control. Positions of *E(spl)-C* primers are shown in Fig 3A; the remaining primers are control non-Notch-responsive regions. Mean, n = 2.

B *brm* RNAi reduces nucleosome turnover at Notch-responsive regions. CATCH-IT-qPCR results as in A after *brm* or *lacZ* RNAi as a control. Mean +/- SEM; n = 5; * p<0.05 with one-tailed student's t-test comparing *brm* and *lacZ* RNAi.

C Brm is required for Notch-responsive nucleosome turnover. CATCH-IT-qPCR results after *brm* or *lacZ* RNAi as in B and pMT-NICD expression as in A. Mean +/- SEM; n=3; * p<0.05 with two-tailed student's t-test compared to control (*lacZ* RNAi Notch-ON bars are compared to *lacZ* RNAi Notch-OFF bars and *brm* RNAi bars are compared to their respective *lacZ* RNAi control bars).

D *brm* RNAi reduces incorporation of histone H3.3. V5 ChIP-qPCR in Kc167 cells after *lacZ* or *brm* RNAi treatment in cells with H3-V5 or H3.3-V5 expression induced from the pMT promoter by 3 hours of copper treatment, shown as fold enrichment over input samples. Mean +/- SEM; n = 3. * p<0.05 with two-tailed Welch's t-test compared to *lacZ* RNAi control.

Figure 6 - Model of BRM complex action.

A In the absence of Notch signaling, the BRM complex maintains the accessibility of Notch-responsive enhancers to allow Su(H) recruitment by promoting nucleosome turnover.

B When Notch signaling is activated, the nucleosome turnover at Notch-responsive enhancers increases, increasing the accessibility of the chromatin and allowing more Su(H) to bind. The BRM complex is essential for the process to occur. Target genes are activated via co-activators.

Expanded View Figure Legends

Figure EV1 - Histone H3.3 is incorporated dynamically at the *E(spl)-C* in Notch-ON nuclei.

A Live imaging of H3.3-GFP (green), H3.3-mKO (magenta) and ParB-mCherry (cyan) expressed in larval salivary gland nuclei using 1151-Gal4 with the *UAS-FRT-H3.3-GFP-PolyA-FRT-H3.3-mKO-PolyA* transgene [34]. H3.3-mKO expression was initiated by heat shock-inducible flippase expression approximately 24 hours before imaging (see Methods for details), and ParB-mCherry indicates the *E(spl)-C* as in Fig 1. H3.3-mKO incorporation shows a similar pattern to H3.3-GFP in Notch-OFF (LacZ expression) and Notch-ON ($N^{\Delta ECD}$ expression) nuclei, as higher levels are present relative to surrounding regions in the Notch-ON condition. Yellow arrow indicates position of *E(spl)-C* on chromosome. Scale bars (white) = 5 µm.

B Quantifications of relative fluorescence intensity of H3.3-GFP, H3.3-mKO and ParB-mCherry across the *E(spl)-C* in Notch-OFF (upper) and Notch-ON (lower) conditions. Mean+/-SEM; n_{nuclei} = 3, 5 and n_{glands} = 3, 3 where each gland represents a biological replicate (from top to bottom).

Figure EV2 - The RNAi lines used successfully reduce RNA and protein levels.

A, B Effects of the indicated RNAi expression in salivary glands on cDNA levels, measured by reverse transcription-qPCR; percentage cDNA compared to *w* RNAi control after normalizing to an internal control for each sample (*RpL32* for most but *RpII215* for *Moira* as *Moira* RNAi appeared to affect *RpL32* levels). All reduce their respective cDNA levels, with *polybromo* RNAi causing a greater reduction than *Snr1*, despite not having an effect on Su(H) recruitment (B). Note that samples included RNA extracted from adjoining fat cells as well as salivary glands, and thus some variability in the knockdowns is attributed to residual expression of chromatin remodelers and chaperones in the fat tissue where the RNAi was not expressed. Mean, n = 2.

C Live Hoechst 33342 staining (blue) of salivary glands expressing either *w* RNAi or BrmK804R. Chromosomes are observed with distinctive banding patterns under both conditions despite chromosomes being slightly smaller with BrmK804R expression. Scale bars (white) = 5 µm.

D, F Immunofluorescence staining of OSA (C; magenta) and BAP170 (E; magenta) in salivary glands expressing *osa* (stock (2) in Fig 2) and *Bap170* RNAi respectively, compared to *w* RNAi control glands. *osa* RNAi depletes all detectable OSA protein and *Bap170* RNAi removes most BAP170 protein. Yellow arrows indicate salivary gland nuclei and yellow arrowheads indicate fat cell nuclei for comparison where RNAi is not expressed. Scale bars (white) = 50 µm.

E, G Quantifications of OSA (E) and BAP170 (G) nuclear levels from maximum projection images with salivary gland nuclei normalized to fat cell nuclei.

Figure EV3 - The effects of BrmK804R on the accessibility and expression of Notch-inducible genes are not widespread.

A, B Chromatin accessibility in Notch-OFF (A) and Notch-ON ($N^{\Delta ECD}$ expression, B) salivary gland nuclei measured by ATAC-qPCR; fold enrichment at the indicated regions compared to a "closed ctrl" region. Expression of dominant-negative Brm, BrmK804R, had little effect or increased the accessibility of some regions. "Hsp26 tr" and "Hsp70 enh" are heat shock-responsive regions, while "Hr4 enh", "Dip-B tr" and "Eip75B" are ecdysone-responsive. "Rab11 tr", "Eip78C", "Closed ctrl" and "Mst87F tr" are the same as shown in Fig 3B and C. Mean +/- SEM; n = 3.

C Effect of Notch activation ($N^{\Delta ECD}$ versus LacZ expression) and BrmK804R expression on gene expression in salivary glands measured by reverse transcription-qPCR. Genes shown are Notch-responsive *E(spl)mβ-HLH* (mβ) and *E(spl)mα-HLH* (mα), housekeeping gene *RpII215,* and ecdysone-responsive *Dip-B* and *Eip75B*. Out of those shown, BrmK804R expression only reduces the Notch-responsive expression of *E(spl)mβ-HLH* and *E(spl)mα-HLH.* Mean, n = 2.

D Effect of *Su(H)* RNAi expression on Su(H)-GFP levels detected with live imaging compared to LacZ expression control. No Su(H)-GFP was left detectable and this genotype was used for the ATAC experiment in Fig 3D. Scale bars (yellow) = 50 µm.

E An acute Notch response in Kc167 cells involves increased enhancer accessibility. Chromatin accessibility across the *E(spl)-C* in Notch-ON (EGTA-treated) and Notch-OFF (PBS control) Kc167 cells detected by ATAC-qPCR. Fold enrichment of the indicated regions compared to a "closed ctrl" region; positions of *E(spl)-C* primers in the genome are shown in Fig 3A. "CTPsyn tr", "fru tr", "kay tr" and "vri tr" are highly accessible control regions which do not respond to Notch. Mean +/- SEM; n = 3.

Figure EV4 - Notch activation does not affect the distribution of histones H3 and H3.3.

A H3-V5 and H3.3-V5 expression in stable cell lines compared to un-transfected "Kc cells", demonstrated by Western blots probed with H3 and V5 antibodies. V5-tagged histones have a larger molecular weight and are not detectable in the H3 blot due to low levels of expression in comparison to endogenous H3.

B, C Effect of Notch activation by EGTA (B) or copper-inducible NICD expression (C) on expression of *E(spl)mβ-HLH* and *E(spl)m3-HLH* in stable cell lines expressing H3-V5 and H3.3-V5, measured by reverse transcription-qPCR. Both methods of activation strongly induce both genes. "N-On" denotes EGTA or copper treatment and "N-Off" denotes PBS alone or no copper.

D, E Notch activation does not affect H3 and H3.3 levels across the *E(spl)*-C. V5 ChIP-qPCR in Kc cells expressing H3-V5 or H3.3-V5 from a ubiquitous promoter with Notch signaling activated by EGTA (D) or 6 hours of copper-inducible NICD expression (E), shown as fold

enrichment over input samples. H3-V5 and H3.3-V5 show a differential pattern across the *E(spl)-C* but Notch activation causes no detectable change in levels compared to controls treated with PBS (D) or no copper (E). Mean +/- SEM, n = 3 (D); Mean, n = 2 (E).

F V5 ChIP-qPCR in Kc cells expressing H3-V5 or H3.3-V5 from a ubiquitous promoter after *lacZ* or *brm* RNAi treatment, shown as fold enrichment over input samples. The changes caused by *brm* RNAi are minimal and do not occur at enhancer regions. Mean +/- SEM; n = 3.

Figure EV5 - Time-course of copper-inducible histone-V5 expression.

A-D V5 ChIP-qPCR in Kc cells with H3-V5 and H3.3-V5 expression induced by copper from the pMT promoter for 60 minutes (A), 90 minutes (B), 3 hours (C) and 24 hours (D), shown as fold enrichment over input samples. Differential incorporation of H3.3 across the *E(spl)-C* is clear after 90 minutes. n = 1 (A and B); mean, n = 2 (C and D).

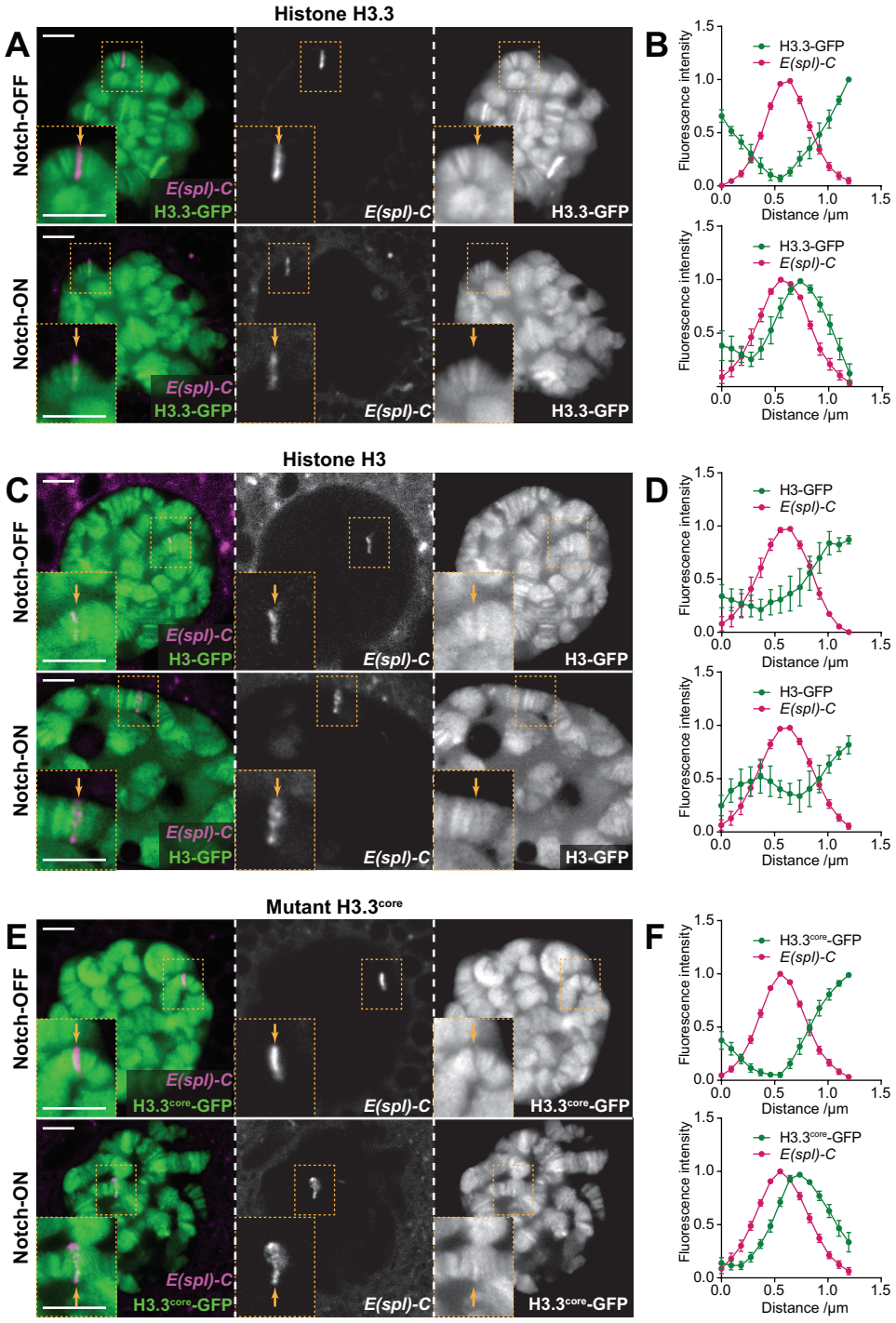
Histone H3.3
A
Notch-OFF
Notch-ON
E(spl)-C
H3.3-GFP
B
H3.3-GFP
E(spl)-C
Fluorescence intensity
Distance /μm
Histone H3
C
H3-GFP
D
Mutant H3.3core
E
H3.3core-GFP
F

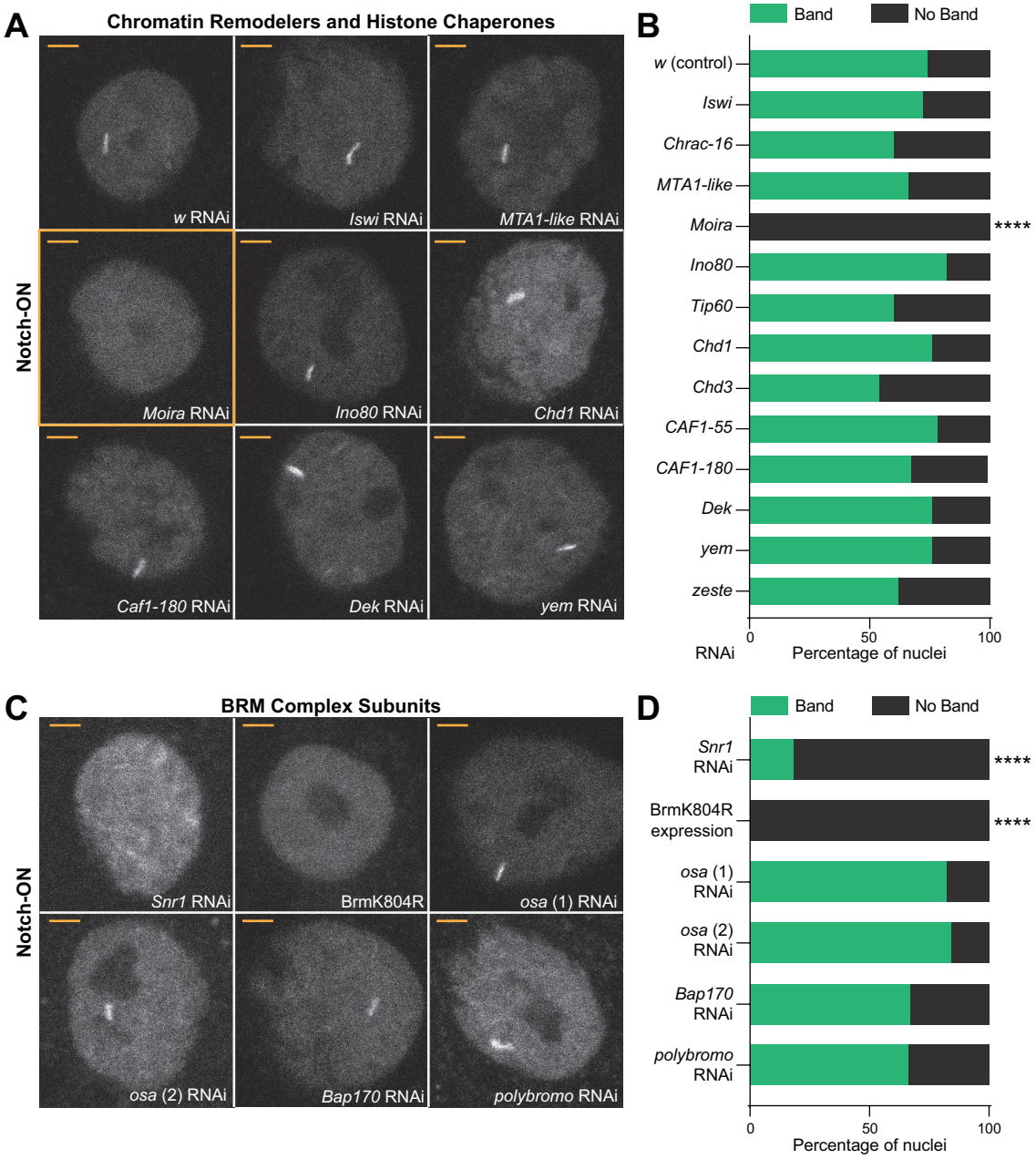
A
Chromatin Remodelers and Histone Chaperones
Notch-ON
w RNAi
Iswi RNAi
MTA1-like RNAi
Moira RNAi
Ino80 RNAi
Chd1 RNAi
Caf1-180 RNAi
Dek RNAi
yem RNAi
B
Band
No Band
w (control)
Iswi
Chrac-16
MTA1-like
Moira
Ino80
Tip60
Chd1
Chd3
CAF1-55
CAF1-180
Dek
yem
zeste
****
0
50
100
RNAi
Percentage of nuclei
C
BRM Complex Subunits
Notch-ON
Snr1 RNAi
BrmK804R
osa (1) RNAi
osa (2) RNAi
Bap170 RNAi
polybromo RNAi
D
Band
No Band
Snr1 RNAi
BrmK804R expression
osa (1) RNAi
osa (2) RNAi
Bap170 RNAi
polybromo RNAi
****
****
0
50
100
Percentage of nuclei

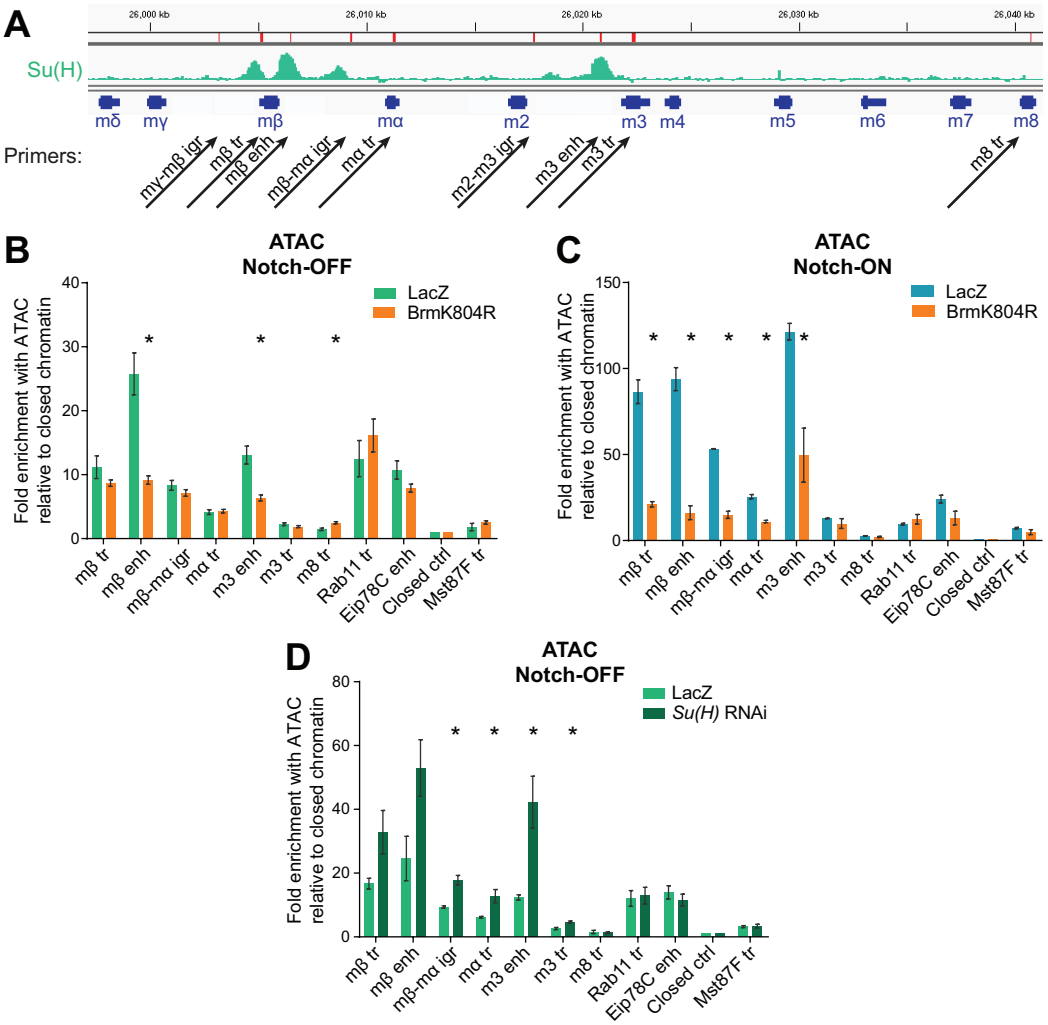
A
26,000 kb
26,010 kb
26,020 kb
26,030 kb
26,040 kb
Su(H)
mδ
mγ
mβ
mα
m2
m3
m4
m5
m6
m7
m8
Primers:
mγ-mβ igr
mβ tr
mβ enh
mβ-mα igr
mα tr
m2-m3 igr
m3 enh
m3 tr
m8 tr
B
ATAC
Notch-OFF
LacZ
BrmK804R
Fold enrichment with ATAC relative to closed chromatin
mβ tr
mβ enh
mβ-mα igr
mα tr
m3 enh
m3 tr
m8 tr
Rab11 tr
Eip78C enh
Closed ctrl
Mst87F tr
C
ATAC
Notch-ON
LacZ
BrmK804R
Fold enrichment with ATAC relative to closed chromatin
D
ATAC
Notch-OFF
LacZ
Su(H) RNAi
Fold enrichment with ATAC relative to closed chromatin

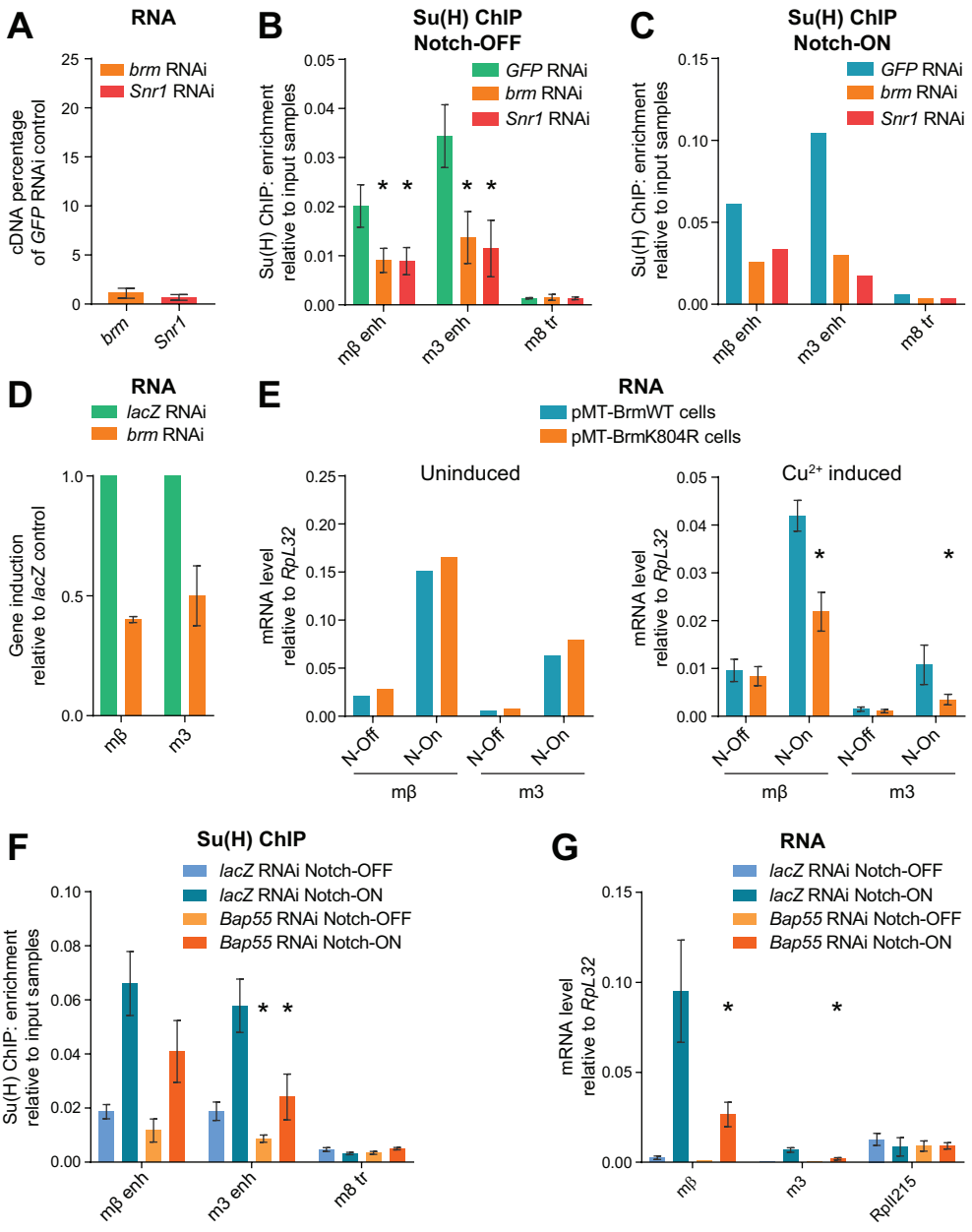
A
RNA
brm RNAi
Snr1 RNAi
cDNA percentage of GFP RNAi control
brm
Snr1
B
Su(H) ChIP
Notch-OFF
GFP RNAi
brm RNAi
Snr1 RNAi
Su(H) ChIP: enrichment relative to input samples
mβ enh
m3 enh
m8 tr
C
Su(H) ChIP
Notch-ON
GFP RNAi
brm RNAi
Snr1 RNAi
Su(H) ChIP: enrichment relative to input samples
mβ enh
m3 enh
m8 tr
D
RNA
lacZ RNAi
brm RNAi
Gene induction relative to lacZ control
mβ
m3
E
RNA
pMT-BrmWT cells
pMT-BrmK804R cells
Uninduced
Cu2+ induced
mRNA level relative to RpL32
N-Off
N-On
mβ
m3
F
Su(H) ChIP
lacZ RNAi Notch-OFF
lacZ RNAi Notch-ON
Bap55 RNAi Notch-OFF
Bap55 RNAi Notch-ON
Su(H) ChIP: enrichment relative to input samples
mβ enh
m3 enh
m8 tr
G
RNA
lacZ RNAi Notch-OFF
lacZ RNAi Notch-ON
Bap55 RNAi Notch-OFF
Bap55 RNAi Notch-ON
mRNA level relative to RpL32
mβ
m3
RpII215

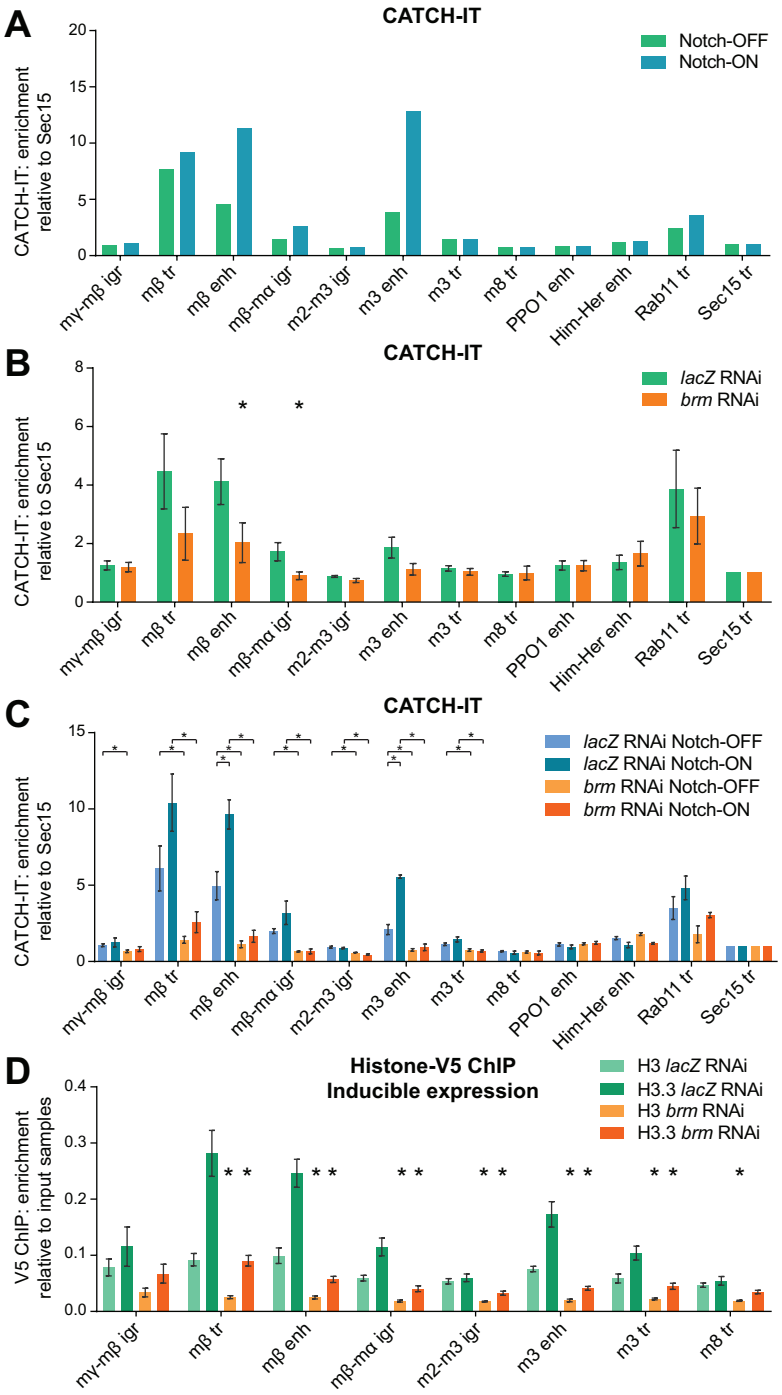
A
CATCH-IT
Notch-OFF
Notch-ON
CATCH-IT: enrichment relative to Sec15
20
15
10
5
0
my-mβ igr
mβ tr
mβ enh
mβ-mα igr
m2-m3 igr
m3 enh
m3 tr
m8 tr
PPO1 enh
Him-Her enh
Rab11 tr
Sec15 tr
B
CATCH-IT
lacZ RNAi
brm RNAi
CATCH-IT: enrichment relative to Sec15
8
6
4
2
0
*
*
my-mβ igr
mβ tr
mβ enh
mβ-mα igr
m2-m3 igr
m3 enh
m3 tr
m8 tr
PPO1 enh
Him-Her enh
Rab11 tr
Sec15 tr
C
CATCH-IT
lacZ RNAi Notch-OFF
lacZ RNAi Notch-ON
brm RNAi Notch-OFF
brm RNAi Notch-ON
CATCH-IT: enrichment relative to Sec15
15
10
5
0
my-mβ igr
mβ tr
mβ enh
mβ-mα igr
m2-m3 igr
m3 enh
m3 tr
m8 tr
PPO1 enh
Him-Her enh
Rab11 tr
Sec15 tr
D
Histone-V5 ChIP
Inducible expression
H3 lacZ RNAi
H3.3 lacZ RNAi
H3 brm RNAi
H3.3 brm RNAi
V5 ChIP: enrichment relative to input samples
0.4
0.3
0.2
0.1
0.0
* *
* *
* *
* *
* *
* *
*
my-mβ igr
mβ tr
mβ enh
mβ-mα igr
m2-m3 igr
m3 enh
m3 tr
m8 tr

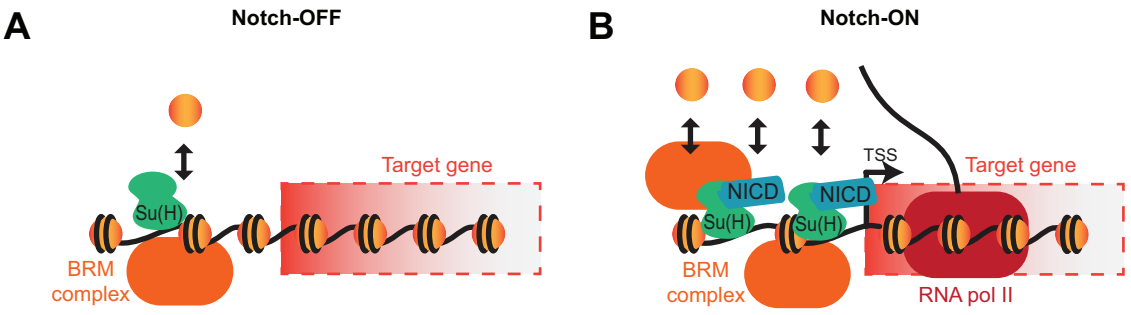
A
Notch-OFF
Target gene
Su(H)
BRM
complex
B
Notch-ON
TSS
Target gene
NICD
NICD
Su(H)
Su(H)
BRM
complex
RNA pol II

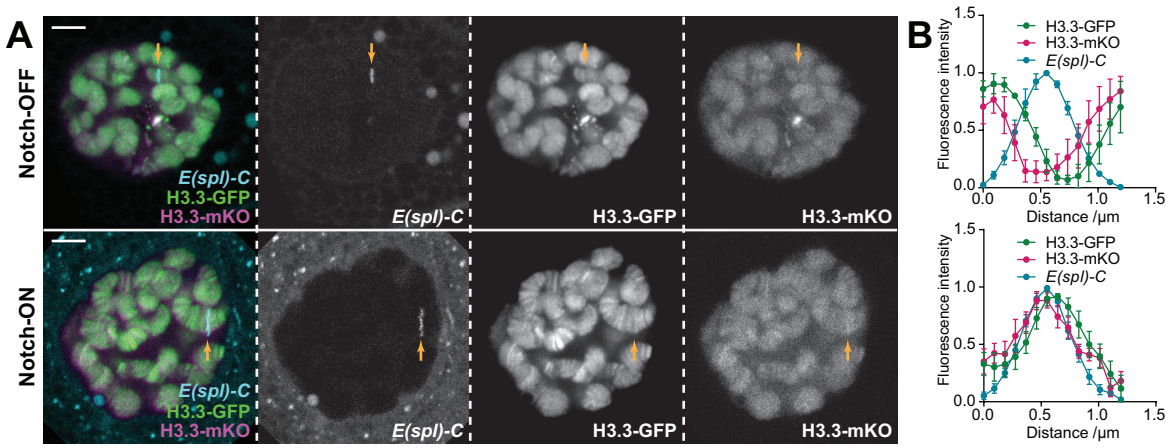
A
Notch-OFF
Notch-ON
E(spl)-C
H3.3-GFP
H3.3-mKO
E(spl)-C
H3.3-GFP
H3.3-mKO
B
Fluorescence intensity
Distance /μm
H3.3-GFP
H3.3-mKO
E(spl)-C
0.0
0.5
1.0
1.5

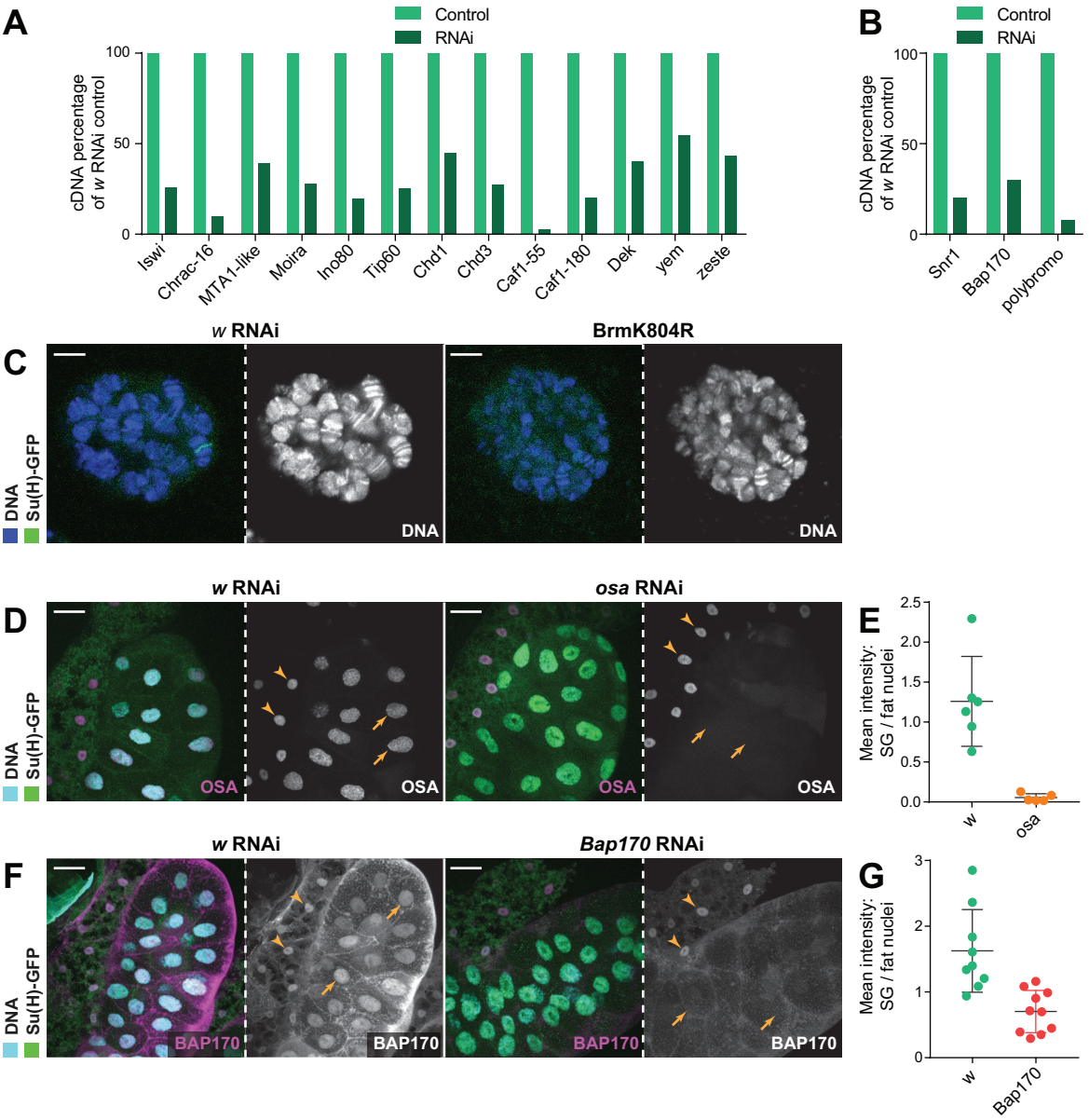
A
Control
RNAi
cDNA percentage of w RNAi control
100
50
0
Iswi
Chrac-16
MTA1-like
Moira
Ino80
Tip60
Chd1
Chd3
Caf1-55
Caf1-180
Dek
yem
zeste
B
Control
RNAi
cDNA percentage of w RNAi control
100
50
0
Snr1
Bap170
polybromo
C
w RNAi
BrmK804R
DNA
Su(H)-GFP
DNA
DNA
D
w RNAi
osa RNAi
DNA
Su(H)-GFP
OSA
OSA
OSA
OSA
E
Mean intensity: SG / fat nuclei
2.5
2.0
1.5
1.0
0.5
0.0
w
osa
F
w RNAi
Bap170 RNAi
DNA
Su(H)-GFP
BAP170
BAP170
BAP170
BAP170
G
Mean intensity: SG / fat nuclei
3
2
1
0
w
Bap170

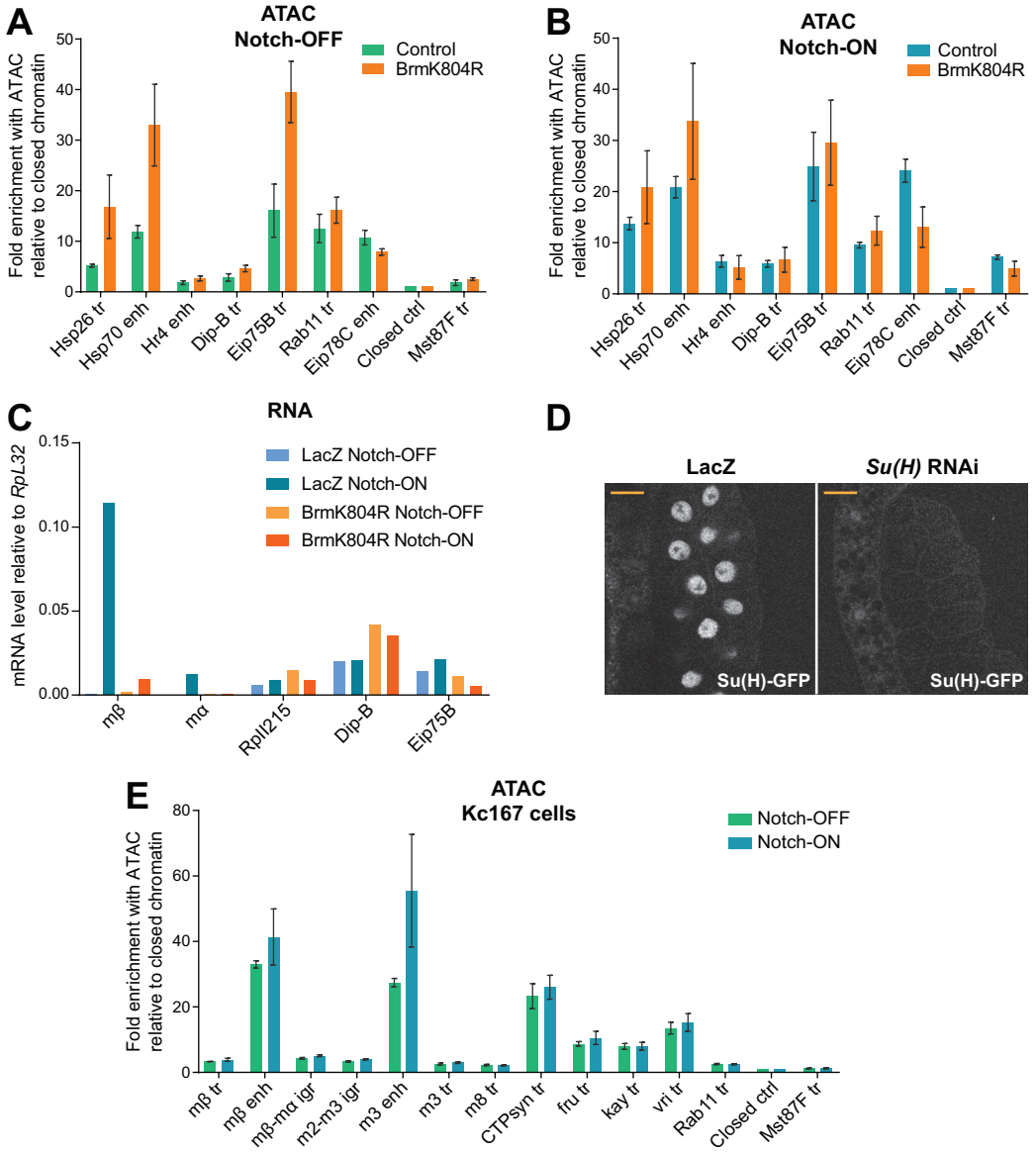
A
ATAC
Notch-OFF
Control
BrmK804R
Fold enrichment with ATAC relative to closed chromatin
0
10
20
30
40
50
Hsp26 tr
Hsp70 enh
Hr4 enh
Dip-B tr
Eip75B tr
Rab11 tr
Eip78C enh
Closed ctrl
Mst87F tr
B
ATAC
Notch-ON
Control
BrmK804R
Fold enrichment with ATAC relative to closed chromatin
0
10
20
30
40
50
Hsp26 tr
Hsp70 enh
Hr4 enh
Dip-B tr
Eip75B tr
Rab11 tr
Eip78C enh
Closed ctrl
Mst87F tr
C
RNA
LacZ Notch-OFF
LacZ Notch-ON
BrmK804R Notch-OFF
BrmK804R Notch-ON
mRNA level relative to RpL32
0.00
0.05
0.10
0.15
mβ
mα
RpII215
Dip-B
Eip75B
D
LacZ
Su(H) RNAi
Su(H)-GFP
Su(H)-GFP
E
ATAC
Kc167 cells
Notch-OFF
Notch-ON
Fold enrichment with ATAC relative to closed chromatin
0
20
40
60
80
mβ tr
mβ enh
mβ-mα igr
m2-m3 igr
m3 enh
m3 tr
m8 tr
CTPsyn tr
fru tr
kay tr
vri tr
Rab11 tr
Closed ctrl
Mst87F tr

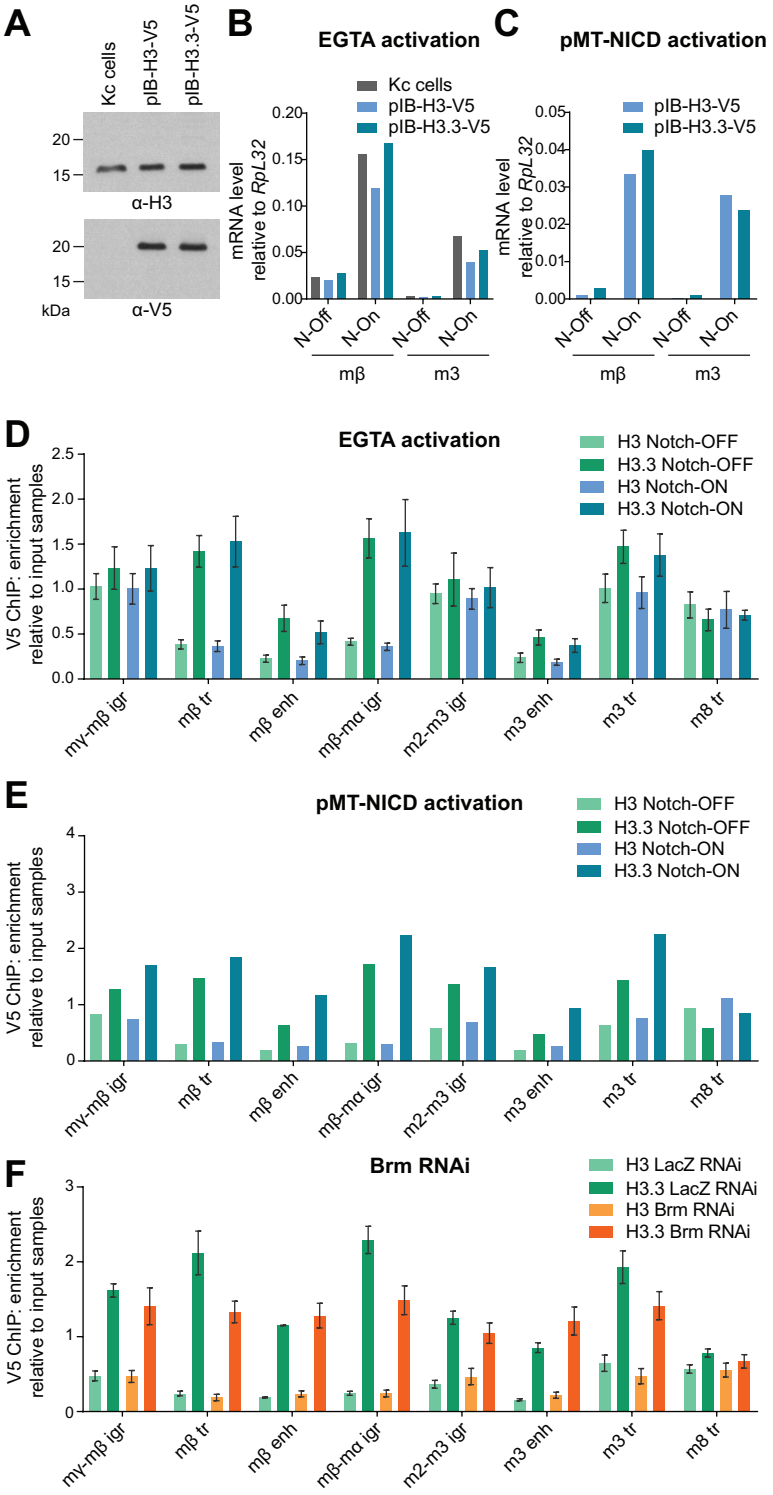
A
Kc cells
pIB-H3-V5
pIB-H3.3-V5
20
15
α-H3
20
15
kDa
α-V5
B
EGTA activation
Kc cells
pIB-H3-V5
pIB-H3.3-V5
mRNA level relative to RpL32
0.20
0.15
0.10
0.05
0.00
N-Off
N-On
N-Off
N-On
mβ
m3
C
pMT-NICD activation
pIB-H3-V5
pIB-H3.3-V5
mRNA level relative to RpL32
0.05
0.04
0.03
0.02
0.01
0.00
N-Off
N-On
N-Off
N-On
mβ
m3
D
EGTA activation
H3 Notch-OFF
H3.3 Notch-OFF
H3 Notch-ON
H3.3 Notch-ON
V5 ChIP: enrichment relative to input samples
2.5
2.0
1.5
1.0
0.5
0.0
mγ-mβ igr
mβ tr
mβ enh
mβ-mα igr
m2-m3 igr
m3 enh
m3 tr
m8 tr
E
pMT-NICD activation
H3 Notch-OFF
H3.3 Notch-OFF
H3 Notch-ON
H3.3 Notch-ON
V5 ChIP: enrichment relative to input samples
4
3
2
1
0
mγ-mβ igr
mβ tr
mβ enh
mβ-mα igr
m2-m3 igr
m3 enh
m3 tr
m8 tr
F
Brm RNAi
H3 LacZ RNAi
H3.3 LacZ RNAi
H3 Brm RNAi
H3.3 Brm RNAi
V5 ChIP: enrichment relative to input samples
3
2
1
0
mγ-mβ igr
mβ tr
mβ enh
mβ-mα igr
m2-m3 igr
m3 enh
m3 tr
m8 tr

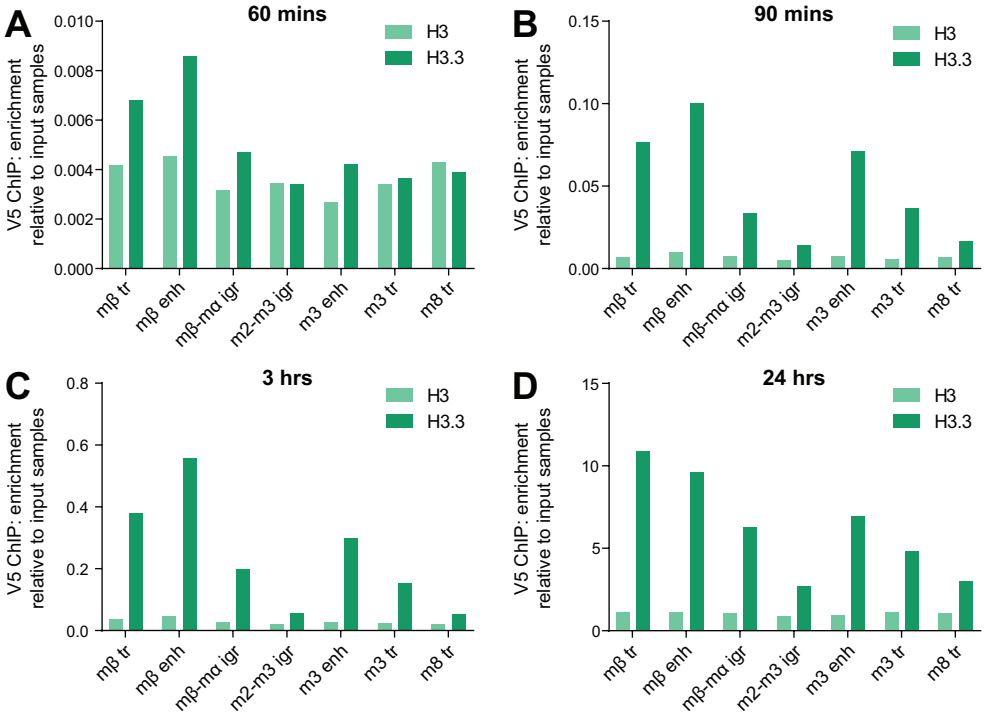
A
60 mins
H3
H3.3
V5 ChIP: enrichment relative to input samples
0.010
0.008
0.006
0.004
0.002
0.000
mβ tr
mβ enh
mβ-mα igr
m2-m3 igr
m3 enh
m3 tr
m8 tr
B
90 mins
H3
H3.3
V5 ChIP: enrichment relative to input samples
0.15
0.10
0.05
0.00
mβ tr
mβ enh
mβ-mα igr
m2-m3 igr
m3 enh
m3 tr
m8 tr
C
3 hrs
H3
H3.3
V5 ChIP: enrichment relative to input samples
0.8
0.6
0.4
0.2
0.0
mβ tr
mβ enh
mβ-mα igr
m2-m3 igr
m3 enh
m3 tr
m8 tr
D
24 hrs
H3
H3.3
V5 ChIP: enrichment relative to input samples
15
10
5
0
mβ tr
mβ enh
mβ-mα igr
m2-m3 igr
m3 enh
m3 tr
m8 tr